A Passive-Impedance-Matching Technology to Achieve Automatic Current Sharing for a Multiphase Resonant Converter

Hongliang Wang, *Senior Member, IEEE*, Yang Chen, *Student Member, IEEE*, and Yan-Fei Liu, *Fellow, IEEE*

***Abstract*—A passive-impedance-matching (PIM) technology is proposed to achieve automatic current sharing for multiphase resonant converters through matching the input impedance of each phase. The series inductors (or series capacitors) of each phase are connected in parallel to achieve a couple of virtual resistors including positive and negative resistors and variably series inductors (or capacitors). A virtual positive (or negative) resistor increases (or decreases) the input impedance of the respective phase, and the variably series inductors can also compensate the component tolerance such that the impedance of each phase is matched. The current-sharing performance of the common-inductor two-phase LLC resonant converter (as one example) is evaluated under the first-harmonic-approximation assumption. The virtual positive and negative resistors and variably virtual inductors are calculated. The proposed method can share the primary resonant current and the load current for all phases without any additional circuit and control strategy. The PIM technology is extended to other resonant converter topologies, including common-inductor or common-capacitor series-resonant converter, LCC, CLL resonant converter, etc. A 600-W 12-V common-inductor two-phase LLC resonant converter prototype is built to verify the feasibility and demonstrate advantages of PIM technology.**

***Index Terms*—Current-sharing error, multiphase LLC, passive impedance matching (PIM), resonant converter.**

I. Introduction

An LLC resonant converter has been widely used due to its high efficiency and zero-voltage switching (ZVS) on the primary-side MOSFETs and zero-current switching (ZCS) on the secondary-side diodes [1], [2]. The related analysis and design methods can be found in [3]–[15]. For high-power applications, current stress of power devices increases with the power rating, so the multiphase parallel technique is a good choice to solve this problem [16]–[18]. However, component tolerances will cause different resonant frequencies among LLC phases [19]–[21]. This will lead to the deviation of current stress in each LLC phase. Small component tolerances will also cause a large current imbalance. It is demonstrated in [22] that one phase with $\pm 10\%$ tolerance for the resonant capacitors may supply all the output current, while another phase does not supply output current at all.

Three techniques have been used to achieve current sharing in a multiphase LLC converter. The first is the active method, in which passive component tolerance can be compensated independently by adjusting the equivalent resonant capacitor [19], [23] or the equivalent resonant inductor [24] with an additional circuit. This technique achieves prefect load-sharing performance, but it has disadvantages of high cost, complex control, and nonexcellent dynamic performance due to sensing of the circulating current and control of the additional switches. The second one is of self-balanced dc voltage based on series bus capacitors [21], [25], [26]. The mid-point voltage is changed due to the difference between two phases' output power. The equivalent input voltage of each phase is adjusted to change voltage gain. Thus, it has advantages of low cost and achieves good load current-sharing performance. However, it has poor reliability because the dc gain is halved when one phase is broken. Besides, it is hard for the modularization design since the dc voltage stress is reduced with the increasing module number. The gate drive circuit for the top phase becomes complicated. The third one is of a three-phase three-wire structure for a three-phase LLC converter based on the 120° phase shift, which has good load current-sharing performance around resonant frequency [27], [28]. However, it is only suitable for three LLC modules in parallel. The load current will not share very well when the number of parallel modules is more than three.

From the above review, it is noted that the existing techniques cannot achieve cost-effective flexible current-sharing performances for multiphase LLC resonant converters. All three methods are defined as the decoupled multiphase resonant converter because the resonant tanks of each phase are decoupled.

Recently, the authors have proposed the coupled multiphase resonant converter [29]–[33], in which the several components of each phase resonant tank are shared; two realization methods are used to construct the common-inductor two-phase LLC resonant converter [29] and the common-capacitor two-phase LLC resonant converter [30]. This technology is simple; neither additional components nor complex control techniques are needed. It can be expanded to any number of phases.

In this paper, the passive-impedance-matching (PIM) concept is proposed to unify the common-inductor method and the

Manuscript received August 14, 2016; revised November 22, 2016; accepted January 9, 2017. Date of publication January 16, 2017; date of current version August 2, 2017. Recommended for publication by Associate Editor A. Oliver.

The authors are with the Department of Electrical and Computer Engineering, Queen's University, Kingston, ON K7L 3N6 Canada (e-mail: hongliang.wang@queensu.ca; yang.chen@queensu.ca; yanfei.liu@queensu.ca).

Color versions of one or more of the figures in this paper are available online at http://ieeexplore.ieee.org.

Digital Object Identifier 10.1109/TPEL.2017.2653081

common-capacitor method. It emphasizes on the mechanism why they can achieve good current-sharing performance. And the PIM concept is extended into a multiphase (such as three-phase) resonant converter, and other resonant converters, such as series-resonant converter (SRC), parallel-resonant converter, LCC, etc.

This paper analyzes the current-sharing characteristics of the common-inductor and common-capacitor LLC converters. It reveals that by common-inductor or common-capacitor connection, a positive virtual resistor has been added into the phase that would provide more current, and a negative virtual resistor has been added into the phase that would provide less current. The end result is much improved resonant current and load current sharing between two phases. This method is different from the other technologies, where active components are needed. Therefore, this method is called PIM technology to show and emphasize that the resonant tank currents between two phases are shared by matching the impedance of the two resonant tanks through the passive method. The concept of PIM will also be applied to other types of resonant converters. An experimental prototype has been built to demonstrate the effectiveness of the PIM technology.

This paper is organized as follows. Section II introduces the principle of PIM. Section III shows the virtual impedance analysis of a common-inductor two-phase LLC resonant converter. Section IV introduces the extension of the PIM technology. The simulation results are shown in Section V. Section VI shows the experimental results. Conclusion is given in Section VII.

II. Principle of PIM

A good design condition for the LLC converter is to select the series-resonant tank to be inductive so that the LLC converter operates at ZVS at primary side and ZCS at secondary side. Two LLC converters are operated independently with the following general assumptions:

1) two LLC converters operate independently (resonant inductors not connected together);
2) the resonant capacitor, C_{r2}, in converter 2 is 5% larger than the resonant capacitor, C_{r1}, in converter 1, $C_{r2} = 1.05\ C_{r1}$. All the other parameters are same;
3) the switching frequency, input voltage, and output voltage/currents are all same for these two converters;
4) fundamental harmonic assumption (FHA) is used.

The switching frequency is lower than resonant frequency in the LLC converter. The input impedance of converter 1 (or converter 2) is resistive–inductive to guarantee the ZVS performance of primary-side switches. All parameters are same except resonant capacitor $C_{r2} = 1.05\ C_{r1}$. The input impedance is inductive type to guarantee the ZVS performance of the primary-side switches. Thus, the magnitude of the input impedance of converter 1 is smaller than that of converter 2. The phase angle of input impedance of converter 1 lags the input impedance of converter 2.

Then, the following can be observed:

1) the series-resonant impedance of converter 1 is less inductive than that of converter 2;

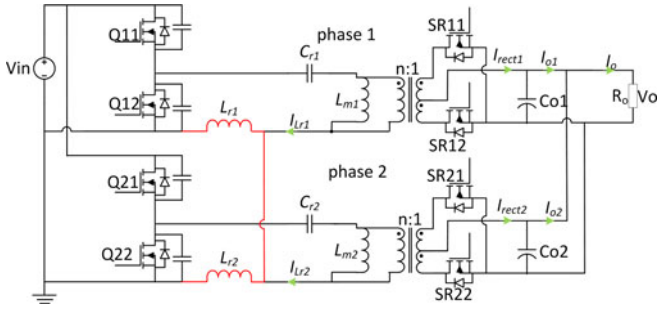

Fig. 1. Circuit diagram of the two-phase common-inductor LLC converter.

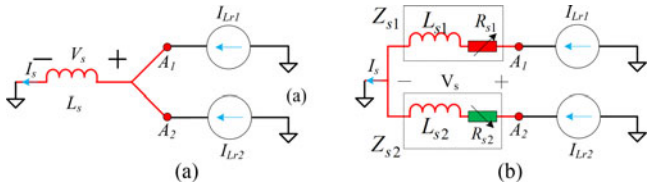

Fig. 2. Transformation from a single inductor to two branches. (a) Common inductor. (b) Equivalent circuit of common inductor.

2) the resonant current in converter 1, I_{Lr1}, will lead the resonant current in converter 2, I_{Lr2};
3) the value of the series impedance in converter 1 will be less than that in converter 2;
4) the value of the resonant current in converter 1 will be larger than that in converter 2.

Two LLC converters are connected in parallel and connect the resonant inductors in parallel, as shown in Fig. 1. By connecting two resonant inductors in parallel, the operation of two resonant tanks is coupled. This section will decouple the operation of these two phases and illustrate how the common-inductor connection can improve the current-sharing performance.

Fig. 2 shows the transformation from a single inductor to two branches. The equivalent circuit of the two-phase common-inductor LLC converter is shown in Fig. 2(a), where I_{Lr1} and I_{Lr2} are the resonant currents through phases 1 and 2, respectively, L_s is a combination of two resonant inductors (L_{r1} and L_{r2}), V_s is the voltage across L_s, and I_s is the current through L_s.

The total resonant inductance L_s is shown as

$$L_s = \frac{L_{r1}L_{r2}}{L_{r1} + L_{r2}}. \tag{1}$$

Based on the circuit theory [33], the circuit shown in Fig. 2(a) can be expressed equivalently, as shown in Fig. 2(b). The single inductor L_s is split into two impedances (Z_{s1} and Z_{s2}). The current I_{Lr1} flows through Z_{s1} and I_{Lr2} flows through Z_{s2}. The voltages at points A_1 and A_2 are the same.

The impedances of Z_{s1} and Z_{s2} can be expressed as

$$\begin{cases} Z_{s1} = R_{s1} + sL_{s1} \\ Z_{s2} = R_{s2} + sL_{s2}. \end{cases} \tag{2}$$

Thus, the single inductor is expressed as

$$\frac{(sL_{s1} + R_{s1})(sL_{s2} + R_{s2})}{s(L_{s1} + L_{s2}) + (R_{s1} + R_{s2})} = sL_s. \tag{3}$$

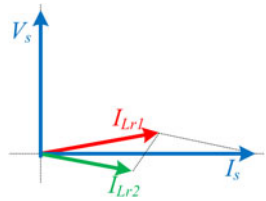

Fig. 3. Phase diagram of I_s, I_{Lr1}, and I_{Lr2}.

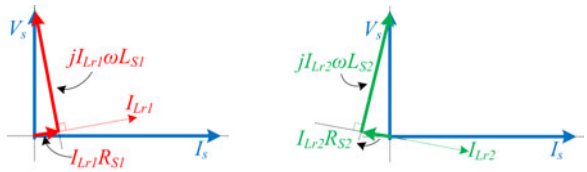

Fig. 4. (a) Phase diagram of V_s, I_s, and I_{Lr1}. (b) Phase diagram of V_s, I_s, and I_{Lr1}.

Therefore, one inductor (L_s) has been separated into two branches: R_{s1}, L_{s1} and R_{s2}, L_{s2}. The current through each branch is the same as the original current, I_{Lr1} and I_{Lr2}.

Due to the component tolerance between these two phases of the LLC converter, the phase and the magnitude of the resonant current, I_{Lr1} and I_{Lr2}, will be different. The current I_s is expressed as

$$I_s = I_{Lr1} + I_{Lr2}. \tag{4}$$

Therefore, the phasor diagram for I_s, I_{Lr1}, and I_{Lr2} can be shown in Fig. 3, where the phase of I_s is used as the reference. It notes that I_{Lr1} and I_{Lr2}, I_{Lr1} leads I_s and I_{Lr2} lags I_s.

The voltage V_s is also calculated by equivalent impedances as

$$V_s = I_{Lr1} * R_{s1} + jI_{Lr1} * \omega L_{s1} \tag{5}$$

$$V_s = I_{Lr2} * R_{s2} + jI_{Lr2} * \omega L_{s2} \tag{6}$$

where ω is the switching frequency. The phase diagrams for (5) and (6) are shown in Fig. 4(a) and (b), respectively.

The phasor diagram shown in Fig. 4(a) shows that R_{s1} is a positive value. It should be emphasized that the phasor diagram shown in Fig. 4(b) indicates that R_{s2} must be a negative value in order to satisfy (4). This is due to the fact that the phase angle between V_s and I_{Lr2} is larger than 90°.

It is known that the phase-angle difference between current I_{Lr1} and current I_{Lr2} results in a pair of virtual resistor R_{s1} and R_{s2}. The virtual resistor is positive for leading current phase and negative for lagging current phase. The positive resistor increases the equivalent input impedance to prevent current further increasing. The negative resistor decreases the equivalent input impedance to prevent current further decreasing.

The inductor L_s can always be split into two impedances in parallel per each phase current I_{Lr1} and I_{Lr2}. The voltage V_s leads less (or more) than $\pi/2$ current I_{Lr1} (or I_{Lr2}). Thus, the equivalent series impedance is the resistor R_{S1} (or R_{S2}) and the inductor L_{s1} (or L_{s2}) in series.

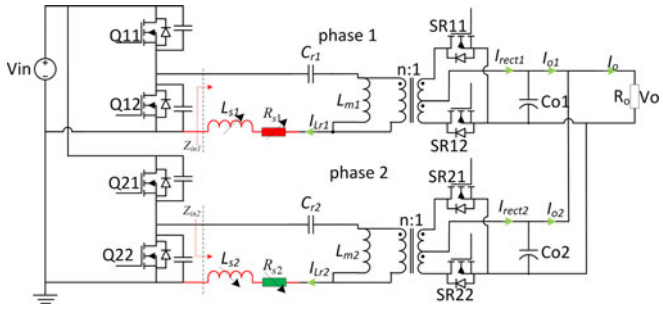

Fig. 5. Decoupled equivalent circuit of the common-inductor LLC converter.

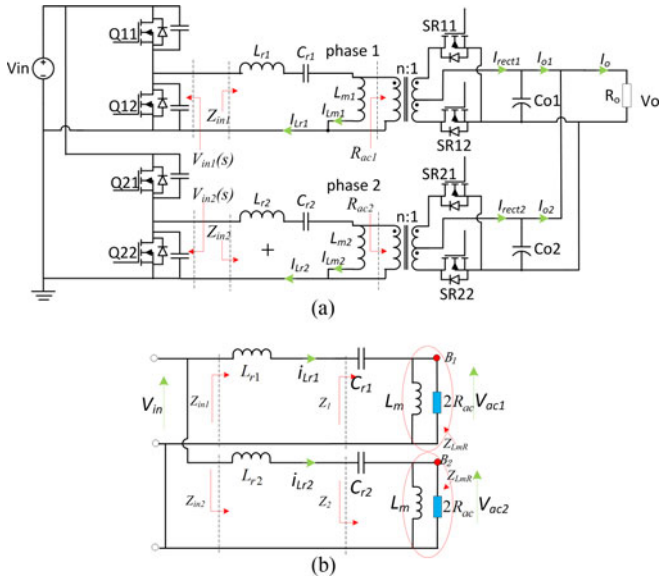

Fig. 6. Conventional LLC converter in parallel. (a) Topology. (b) Equivalent circuit with FHA.

The above analysis shows that by connecting the resonant inductors in two phases in parallel, the operation of the two LLC phases is coupled. The impact of this coupling is equivalent to two components in each phase: a virtual resistor and an equivalent inductor connected in series, as shown in Fig. 5.

More importantly and more helpfully, a positive virtual resistor is added to the phase, which would generate higher current (phase 1 in this case) to reduce the actual resonant current. A negative virtual resistor is added to the phase, which would generate less resonant current (phase 2 in this case). The end result is that the current in two phases is more balanced. They change the equivalent impedance of the resonant tank so that current sharing can be achieved.

In order to illustrate the impact of the virtual resistors and equivalent inductors introduced by the common-inductor connection, the resonant current of each phase is calculated under two cases. One case is that two LLC converters are connected in parallel without a common inductor, the conventional case, as shown in Fig. 6(a). Its FHA equivalent circuit is shown in Fig. 6(b). The other case is the common-inductor case in which the resonant inductors of the two LLC converters are connected

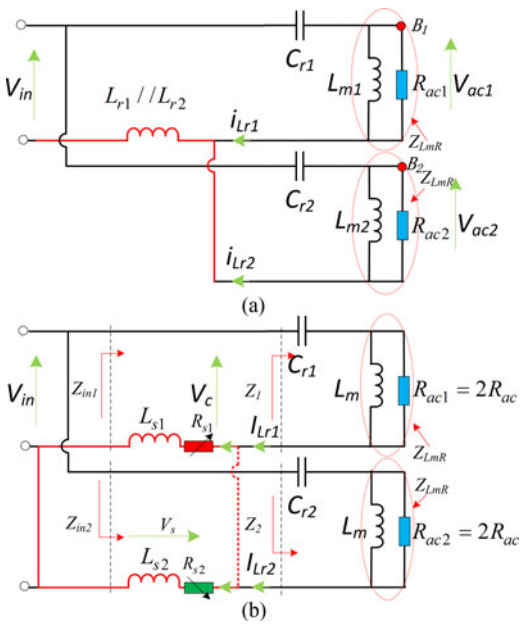

Fig. 7. Common-inductor LLC converter. (a) FHA circuit. (b) Equivalent circuit with FHA.

in parallel, as shown in Fig. 1. Its FHA equivalent circuit is shown in Fig. 7(a).

Fig. 7 shows the common-inductor two-phase LLC converter, in which two resonant inductors are connected. Fig. 7(a) shows the FHA circuit of the common-inductor two-phase LLC resonant converter. The common inductor can be separated into an inductor and a resistor in series. The equivalent circuit with the FHA is shown in Fig. 7(b). In Figs. 6(b) and 7(a), points B1 and B2 do not connect in [31] because the equivalent ac voltages $V_{\rm ac1}$ and $V_{\rm ac2}$ of each phase have the same magnitude, but different phase angle. These FHA circuits are called accurate FHA circuit in this paper.

As the analysis is intended to show the impact of the common inductor on the resonant current, we assume the following:

1) the load resistor is equally split between two phases, $R_{\rm ac1} = R_{\rm ac2} = 2R_{\rm ac}$;
2) $R_{\rm ac}$ is the reflected load resistor, as shown in (7);
3) $C_{\rm r2} = 1.05C_{\rm r1}$, $L_{\rm r2} = L_{\rm r1}$, $L_{\rm m2} = L_{\rm m1}$

$$R_{\rm ac} = \frac{8n^2}{\pi^2}R_o \tag{7}$$

where n is the turns ratio of the transformer and R_o is the load resistor.

The impedances Z_1 and Z_2 are expressed as

$$\begin{cases} Z_1 = \dfrac{sL_m R_{\rm ac1}}{sL_m + R_{\rm ac1}} + \dfrac{1}{sC_{r2}} \\ Z_2 = \dfrac{scL_m R_{\rm ac2}}{scL_m + R_{\rm ac2}} + \dfrac{1}{sC_{r2}}. \end{cases} \tag{8}$$

In the conventional two-phase LLC converter, as shown in Fig. 6(b), the phase angle and the magnitude of impedance Z_1 are smaller than that of Z_2 if there is only resonant capacitor tolerance, such as $C_{r2} = 1.05\,C_{r1}$. Thus, the resonant current I_{Lr1} leads I_{Lr2}, and I_{Lr1} is larger than I_{Lr2}. There are input impedance differences caused by resonant capacitor tolerance.

The resonant current I_{Lr1} leads I_{Lr2}, and I_{Lr1} is larger than I_{Lr2}. Thus, a positive virtual resistor R_{s1} is added to phase 1, which would generate low input impedance to increase the actual input impedance. A negative virtual resistor R_{s2} is added to phase 2, which would generate high input impedance to reduce the input impedance. The end result is that the input impedance in two phases is more balanced, and then, good current sharing is achieved.

From the above assumption, it is noted that the output loads of each phase are the same. In fact, they are different at different total loads, switching frequencies, and component tolerances.

The resonant tank values of phases 1 and 2 are shown as

$$\begin{cases} L_{r1} = L_r, \;\; L_{r2} = aL_r \\ C_{r1} = C_r, \;\; C_{r2} = bC_r \\ L_{m1} = L_m, \;\; L_{m2} = cL_m \end{cases} \tag{9}$$

where symbols a, b, and c indicate that the resonant parameters for these two phases are different.

The load factor k is defined as the ratio of the load power P_{o1} for phase 1 to the total output power P_o. The output powers of each phase are expressed as

$$\begin{cases} P_{o1} = kP_o \\ P_{o2} = (1-k)P_o \end{cases} \tag{10}$$

where P_{o1}, P_{o2}, and P_o are phase 1 output power, phase 2 output power, and the total output power.

The detailed calculation about the load factor k is provided in [31]. The load factor k is expressed as

$$k = \begin{cases} -\frac{C}{B}, & A = 0, B \neq 0 \\ \frac{-B \pm \sqrt{B^2 - 4AC}}{2A}, & A \neq 0, \sqrt{B^2 - 4AC} \geq 0 \end{cases} \text{ and } k \in [0,1] \tag{11}$$

where parameters A, B, and C under the conventional two-phase LLC can be calculated as

$$\begin{aligned} A =& \omega^2(1-b^2)c^2{L_m}^2 - \omega^4(2ab-2b^2)c^2L_r{L_m}^2C_r \\ &+ \omega^6(a^2-1)b^2c^2{L_r}^2{L_m}^2{C_r}^2 \\ B =& -2\omega^2c^2{L_m}^2 + 4\omega^4abc^2L_r{L_m}^2C_r \\ &- 2\omega^6a^2b^2c^2{L_r}^2{L_m}^2{C_r}^2 \\ C =& \omega^2c^2{L_m}^2 - 2\omega^4abc^2L_r{L_m}^2C_r + \omega^6a^2b^2c^2{L_r}^2{L_m}^2{C_r}^2 \\ &+ (1-b^2c^2)R^2 - \omega^2[(2ab-2b^2c^2)L_r \\ &+ (2bc-2b^2c^2)L_m]C_rR^2 \\ &+ \omega^4(ab-bc)[(ab+bc){L_r}^2 + 2bcL_rL_m]{C_r}^2R^2 \end{aligned} \tag{12}$$

where parameters A, B, and C under the common-inductor two-phase LLC can be calculated as

$$\begin{cases} A = \omega^2(1-b^2)c^2{L_m}^2 \\ B = -2\omega^2c^2{L_m}^2 \\ C = \omega^2c^2{L_m}^2 + (1-b^2c^2)R^2 - 2\omega^2(bc-b^2c^2)L_mC_r{R_{ac}}^2. \end{cases} \tag{13}$$

It is noted that the load factor k is effective when k is between 0 and 1. Otherwise, one phase will provide the load power. And the other absorbs the power from load. It is not hopeful in the application.

The input impedance of the conventional two-phase LLC converter can be calculated as

$$\begin{cases} Z_{\text{in}1} = sL_{r1} + \dfrac{1}{sC_{r1}} + \dfrac{sL_{m1}{R_{\text{ac}}}/{k}}{sL_{m1} + {R_{\text{ac}}}/{k}} \\ Z_{\text{in}2} = sL_{r2} + \dfrac{1}{sC_{r2}} + \dfrac{s_{m2}{R_{\text{ac}}}/{1-k}}{sL_{m2} + {R_{ac}}/{1-k}} \\ s = j\omega \\ \omega = 2\pi f_s. \end{cases} \tag{14}$$

The equivalent FHA circuit of the common-inductor two-phase LLC converter is shown in Fig. 7(b); the equivalent impedances of two phases based on virtual open are Z_{s1} and Z_{s2} and can be calculated as

$$\begin{cases} Z_{s1} = \dfrac{V_s}{I_{Lr1}} \\ Z_{s2} = \dfrac{V_s}{I_{Lr2}}. \end{cases} \tag{15}$$

The equivalent impedances Z_{s1} and Z_{s2} can also be calculated as

$$\begin{cases} Z_{s1} = \dfrac{Z_s}{Z_2}(Z_1 + Z_2) \\ Z_{s2} = \dfrac{Z_s}{Z_1}(Z_1 + Z_2). \end{cases} \tag{16}$$

The impedances Z_{s1} and Z_{s2} are separated as a resistor and a inductor in series, which gives

$$\begin{cases} Z_{s1} = R_{s1} + sL_{s1} \\ Z_{s2} = R_{s2} + sL_{s2}. \end{cases} \tag{17}$$

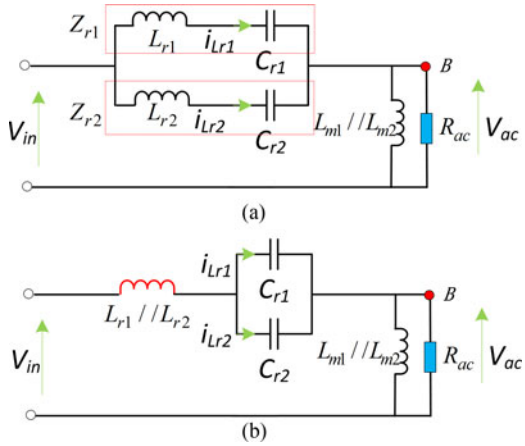

Fig. 8. (a) Simplified FHA circuit of the conventional LLC. (b) Simplified FHA circuit of the common-inductor LLC.

Combining (16) and (17), the relative values of virtual impedances are shown as

$$\begin{cases} {R_{s1}}/{\omega L_s} = -\text{Im}\left(\dfrac{Z_1}{Z_2} + 1\right) \\ {\omega L_{s1}}/{\omega L_s} = \text{Re}\left(\dfrac{Z_1}{Z_2} + 1\right) \\ {R_{s2}}/{\omega L_s} = -\text{Im}\left(\dfrac{Z_2}{Z_1} + 1\right) \\ {\omega L_{s2}}/{\omega L_s} = \text{Re}\left(\dfrac{Z_2}{Z_1} + 1\right). \end{cases} \tag{18}$$

The equivalent input impedance of each phase can be calculated as

$$\begin{cases} Z_{\text{in}1} = Z_{s1} + Z_1 \\ Z_{\text{in}2} = Z_{s2} + Z_2. \end{cases} \tag{19}$$

To evaluate the current-sharing performance, the load current-sharing error σ_{load} is defined in (20), where I_{01} and I_{02} are the dc values of output currents for the two phases

$$\sigma_{\text{load}} = \text{abs}\left(\frac{I_{01} - I_{02}}{I_{01} + I_{02}}\right) = \text{abs}(1-2k), \quad k \in [0,1]. \tag{20}$$

Similarly, the resonant current-sharing error σ_{Resonant} is defined in (21), where $\text{rms}(i_{Lr1})$, $\text{rms}(i_{Lr2})$ are the root-mean-square (RMS) values of resonant currents i_{Lr1} and i_{Lr2}, see (21) set at the bottom of this page.

If the phase-angle difference between point B_1 and point B_2 is neglected as it is small, point B_1 and point B_2 are connected. Two simplified FHA circuits of conventional LLC and common-inductor LLC are shown in Fig. 8.

$$\begin{aligned} \sigma_{\text{Resonant}} &= \text{abs}\left(\frac{\text{rms}(i_{Lr1}) - \text{rms}(i_{Lr2})}{\text{rms}(i_{Lr1}) + \text{rms}(i_{Lr2})}\right) \\ &= \text{abs}\left\{1 - \frac{2c\sqrt{(1-k)^2k^2\omega^4c^4L_m^4 + 2[k^2 + c^2(1-k)^2]\omega^2L_m^2R_{\text{ac}}^2 + R_{\text{ac}}^4}}{(1-2k)\omega^2c^2L_m^2 + (1-c^2)R_{\text{ac}}^2}\right. \end{aligned} \tag{21}$$

In conventional LLC shown in Fig. 8(a), Z_{Cr1} and Z_{Cr2} are the total impedance of the resonant inductor and the resonant capacitor of each phase

$$\begin{cases} Z_{r1} = sL_{r1} + \dfrac{1}{sC_{r1}} \\ Z_{r2} = sL_{r2} + \dfrac{1}{sC_{r2}}. \end{cases} \tag{22}$$

The current-sharing error between i_{Lr1} and i_{Lr2} can be calculated as

$$\sigma_{\text{Resonant}} = \text{abs}\left(\frac{Z_{r2} - Z_{r1}}{Z_{r2} + Z_{r1}}\right) \tag{23}$$

where $|Z_{r1}|$ and $|Z_{r2}|$ are the magnitudes of impedance Z_{r1} and Z_{r2}. When the switching frequency is close to the resonant frequency, Z_{r1} will be close to 0 and, thus, negligible as compared to Z_{r2}. Then, the current-sharing error is almost equal to 1, and there is almost only one phase that provides the total load power.

From Fig. 8(b), the current-sharing error of common-inductor LLC is shown as

$$\sigma_{\text{Resonant}} = \text{abs}\left(\frac{C_{r2} - C_{r1}}{C_{r1} + C_{r2}}\right). \tag{24}$$

The current-sharing error is 5% when the resonant capacitor has 5% tolerance, such as $C_{r2} = 1.05\,C_{r1}$. It is noted that the load current-sharing error is 0 if there is only the tolerance of magnetizing inductance, such as $L_{m2} = 1.05\ L_{m1}$. The load current-sharing error is not accurate in this case. However, the accurate FHA circuits shown in Figs. 6(b) and 7(a) can achieve the accurate load current-sharing error because the phase angle between V_{ac1} and V_{ac2} is different. The detailed analysis will be given in Section III.

III. Analysis of a Common-Inductor Two-Phase LLC Resonant Converter

In this section, a more accurate analysis on the input impedance and virtual resistor and inductor are introduced. It is noted that the ac loads R_{ac1} and R_{ac2} are no longer the same due to component tolerance. A component tolerance of $\pm 5\%$ is considered to analyze the input impedance between the conventional two-phase LLC resonant converter and the common-inductor two-phase LLC resonant converter. The analysis in Section II shows that the input impedance is more balanced for the common-inductor two-phase LLC converter under $C_{r2} = 1.05\ C_{r1}$. The load current-sharing error, the equivalent input impedance, the virtual resistor, and the virtual inductance are calculated from (18)–(20) in Section II. A set of LLC parameters based on the load power of 300 W of each phase is designed and shown in Table I.

The more accurate analysis results are shown in Section III-A. Section III-B shows the more accurate input impedance and virtual resistor and virtual inductor under four corner cases. To evaluate current sharing performance, the parameters can be given with the existing design method [34].

TABLE I
Values of LLC-Related Parameters

Resonant inductor L_r	29 μH
Resonant capacitor C_r	12 nF
Magnetizing inductor L_m	95 μH
Switching frequency fs	160–250 kHz
Transformer ratio n	20
Resonant frequency f_r	270 kHz
Output voltage V_o	12V (rated voltage)
Total output load R_o	Rated load 0.24 Ω

A. Analysis Results Under $C_{r2} = 1.05\ C_{r1}$

Fig. 9 shows the comparison of the input impedance of the conventional two-phase LLC and the common-inductor two-phase LLC under $L_{r2} = L_{r1}$, $C_{r2} = 1.05\ C_{r1}$, $L_{m2} = L_{m1}$, and $R_o = 0.24\,\Omega$. To easy understand the impedance difference, the series inductor and capacitor tolerances are estimated. In the rated load, the output voltage is 12 V when the input voltage equals 380 V at $f_s = 240$ kHz. $+5\%$ L_r tolerance means 2.2-Ω impedance difference, and $+5\%$ Cr tolerance means 0.27-Ω impedance difference at f_s =240 kHz.

Fig. 9(a) and (b) shows Z_{in1} and Z_{in2} of the conventional two-phase LLC resonant converter and the common-inductor two-phase LLC resonant converter, respectively. The input impedance difference between two phases is reduced significantly from the conventional two-phase LLC converter to the common-inductor two-phase LLC converter. For example, when $f_s = 240\,\text{kHz}$, $Z_{\text{in1}} = 62\,\Omega$, and $Z_{\text{in2}} = 132\,\Omega$ for the conventional two-phase LLC converter, the difference of each phase is 70 Ω. However, the input impedance difference is 1 Ω for the common-inductor two-phase LLC converter, as $Z_{\text{in1}} = 99\,\Omega$ and $Z_{\text{in2}} = 100\,\Omega$ at $f_s = 240\,\text{kHz}$.

Fig. 9(c) shows the virtual inductor of the common-inductor two-phase LLC resonant converter: $L_{s1} = 43.7\,\Omega$ and $L_{s2} = 44.4\,\Omega$ at $f_s = 240\,\text{kHz}$. The virtual inductor tolerance is $L_{s2}/L_{s1} = 1.01$ at f_s = 240 kHz. Thus, the common-inductor two-phase LLC converter can almost be equivalent to the two-phase LLC converter under $L_{s2} = 1.01\ L_{s1}$, $C_{r2} = 1.05\ C_{r1}$, and $L_{m2} = L_{m1}$. There is same directional tolerance between the series inductor and the series capacitor. If the virtual resistor is zero between two phases, the input impedance of phase 1 is smaller than the input impedance of phase 2.

A couple of virtual resistors of the common-inductor two-phase LLC converter are shown in Fig. 9(d): $R_{s1} = 1.8\,\Omega$ and $R_{s2} = -1.8\,\Omega$ at $f_s = 240\,\text{kHz}$. A positive resistor R_{s1} is automatically constructed to increase the input impedance of phase 1, and a negative resistor R_{s2} is automatically yield to decrease the input impedance of phase 2. Thus, the input impedances between two phases are more balanced. The current difference can be suppressed.

The above analysis shows that there is input impedance matching owning to virtual resistor's function in this situation.

B. Analysis Results Under Four Corner Cases

The current-sharing performance is good if the series inductor and the capacitor have two different direction tolerances because

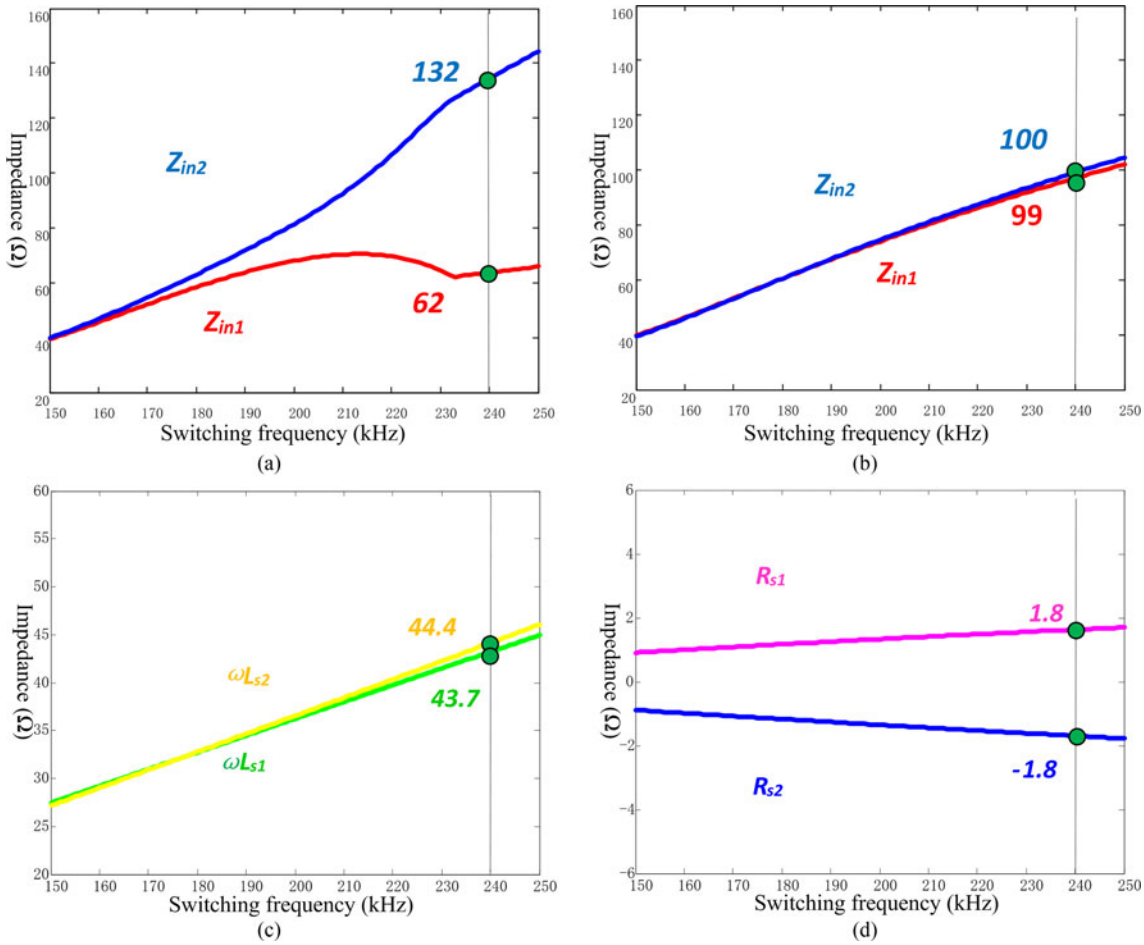

Fig. 9. Input impedance and virtual impedance under $L_{r2} = L_{r1}$, $C_{r2} = 1.05\ C_{r1}$, $L_{m2} = L_{m1}$, and $R_0 = 0.24\Omega$. (a) Input impedance of the conventional LLC. (b) Input impedance of the common-inductor LLC. (c) Virtual inductor of the common-inductor LLC. (d) Virtual resistor of the common-inductor LLC.

the input impedance difference is eliminated between series inductor tolerance and series capacitor tolerance. In other words, the resonant frequencies of each phase are almost the same.

Fig. 10 shows the comparison of the input impedance of the conventional two-phase LLC and the common-inductor two-phase LLC under $L_{r2} = 1.05\ L_{r1}$, $C_{r2} = 1.05\ C_{r1}$, $L_{m2} = 1.05\ L_{m1}$, and $R_o = 0.24\,\Omega$.

Fig. 10(a) and (b) shows $Z_{\text{in}1}$ and $Z_{\text{in}2}$ of the conventional two-phase LLC resonant converter and the common-inductor two-phase LLC resonant converter, respectively. The input impedance magnitude difference of two phases is reduced significantly from the conventional two-phase LLC converter to the common-inductor two-phase LLC converter. For example, when $f_s = 240$ kHz, $Z_{\text{in}1} = 60\,\Omega$, and $Z_{\text{in}2} = 144\,\Omega$ for the conventional two-phase LLC converter, the difference of each phase is 84 Ω. However, the input impedance difference is 6 Ω for the common-inductor two-phase LLC converter, as $Z_{\text{in}1} = 99\,\Omega$ and $Z_{\text{in}2} = 105\,\Omega$.

Fig. 10(c) shows the virtual inductor of the common-inductor two-phase LLC resonant converter: $L_{s1} = 43.5\ \Omega$ and $L_{s2} = 46.5\ \Omega$ at $f_s = 240$ kHz. The virtual inductor tolerance is $L_{s2}/L_{s1} = 1.07$ at $f_s = 240$ kHz. Thus, the common-inductor two-phase LLC can almost be equivalent to the two-phase LLC converter under $L_{s2} = 1.07\ L_{s1}$, $C_{r2} = 1.05\ C_{r1}$, $L_{m2} = 1.05\ L_{m1}$. There is same directional tolerance between the series inductor and the series capacitor. If the virtual resistors R_{s1} and R_{s2} are zero, the equivalent input impedance of phase 1 is smaller than the one of phase 2.

A couple of virtual resistors of the common-inductor two-phase LLC converter are shown in Fig. 10(d): $R_{s1} = 3\,\Omega$ and $R_{s2} = -3.5\,\Omega$ at $f_s = 240$ kHz. A positive resistor R_{s1} is automatically constructed to increase the input impedance of phase 1, and a negative resistor R_{s2} is automatically yield to decrease input impedance of phase 2. The input impedances between two phases are more balanced. The current difference can be suppressed.

The above analysis shows that there is input impedance matching owning to virtual resistor's function in this situation.

Fig. 11 shows the comparison of the input impedance of the conventional two-phase LLC and the common-inductor two-phase LLC under $L_{r2} = 0.95\ L_{r1}$, $C_{r2} = 1.05\ C_{r1}$, $L_{m2} = 1.05\ L_{m1}$, and $R_o = 0.24\,\Omega$.

Fig. 11(a) and (b) shows $Z_{\text{in}1}$ and $Z_{\text{in}2}$ of the conventional two-phase LLC resonant converter and the common-inductor two-phase LLC resonant converter, respectively. Compared with the conventional two-phase LLC, the input impedance

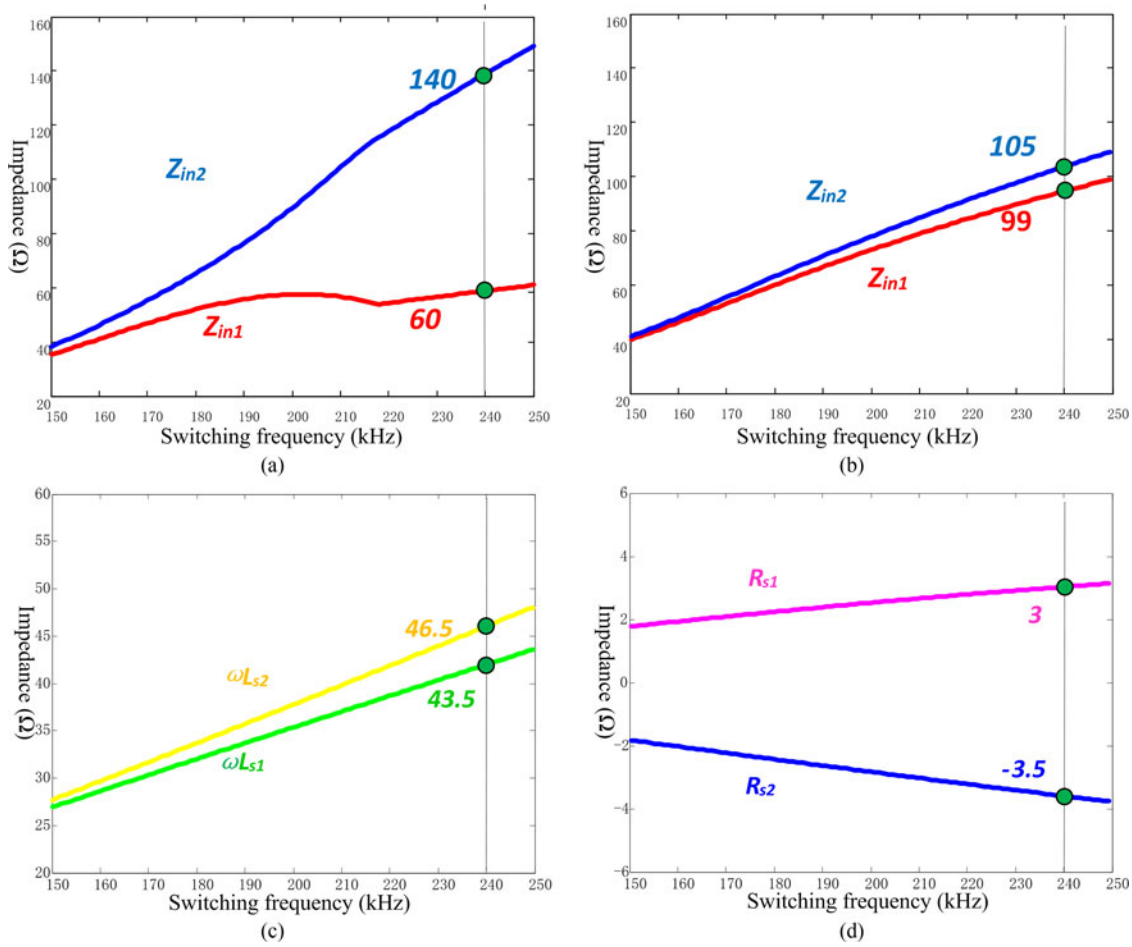

Fig. 10. Input impedance and virtual impedance under $L_{r2} = 1.05\ L_{r1}$, $C_{r2} = 1.05\ C_{r1}$, $L_{m2} = 1.05\ L_{m1}$, and $R_0 = 0.24\,\Omega$. (a) Input impedance of the conventional LLC. (b) Input impedance of the common-inductor LLC. (c) Virtual inductor of the common-inductor LLC. (d) Virtual resistor of the common-inductor LLC.

magnitude difference of two phases is reduced significantly based on the common-inductor two-phase LLC converter. For example, when $f_s = 240$ kHz, $Z_{\text{in}1} = 76\,\Omega$, and $Z_{\text{in}2} = 126\,\Omega$ for the conventional two-phase LLC converter, and $Z_{\text{in}1} = 98\,\Omega$, and $Z_{\text{in}2} = 104\ \Omega$ for the common-inductor two-phase LLC. The difference of each phase is reduced from 50 to 6 Ω.

Fig. 11(c) shows the virtual inductor of the common-inductor two-phase LLC resonant converter: $L_{s1} = 41\,\Omega$ and $L_{s2} = 44\,\Omega$ at $f_s = 240$ kHz. The virtual inductor tolerance is $L_{s2}/L_{s1} = 1.07$. Thus, the common-inductor two-phase LLC can almost be equivalent to the two-phase LLC converter under $L_{s2} = 1.07\ L_{s1}$, $C_{r2} = 1.05\ C_{r1}$, and $L_{m2} = 1.05\ L_{m1}$.

There is same directional tolerance between the series inductor and the series capacitor. The equivalent input impedance of phase 1 is smaller than the one of phase 2 if the virtual resistors R_{s1} and R_{s2} are zero.

A couple of virtual resistors of the common-inductor two-phase LLC converter are shown in Fig. 11(d): $R_{s1} = 3\,\Omega$ and $R_{s2} = -3.5\,\Omega$ at $f_s = 240$ kHz. A positive resistor R_{s1} is automatically constructed to increase the input impedance of phase 1, and a negative resistor R_{s2} is automatically yield to decrease the input impedance of phase 2. Thus, the input impedances between two phases are more balanced. The current difference can be suppressed. The above analysis shows that there is input impedance matching owning to virtual resistor's function in this situation.

Fig. 12 shows the comparison of the input impedance of the conventional two-phase LLC and the common-inductor two-phase LLC under $L_{r2} = 1.05\ L_{r1}$, $C_{r2} = 0.95\ C_{r1}$, $L_{m2} = 1.05\ L_{m1}$, and $R_o = 0.24\,\Omega$.

Fig. 12(a) and (b) shows $Z_{\text{in}1}$ and $Z_{\text{in}2}$ of the conventional two-phase LLC resonant converter and the common-inductor two-phase LLC resonant converter, respectively. The input impedance difference of each phase in Fig. 12(a) is very small, as there are conversely directional tolerances the between series inductor and the series capacitor. In this case, good current-sharing performance is achieved based on the conventional two-phase LLC resonant converter and the common-inductor two-phase LLC resonant converter.

Fig. 12(c) shows the virtual inductor of the common-inductor two-phase LLC resonant converter: $L_{s1} = 44\,\Omega$ and $L_{s2} = 46\,\Omega$ at $f_s = 240$ kHz. The virtual inductor tolerance is $L_{s2}/L_{s1} = 1.05$. Thus, the common-inductor two-phase LLC can almost be equivalent to the two-phase LLC converter under $L_{s2} =$

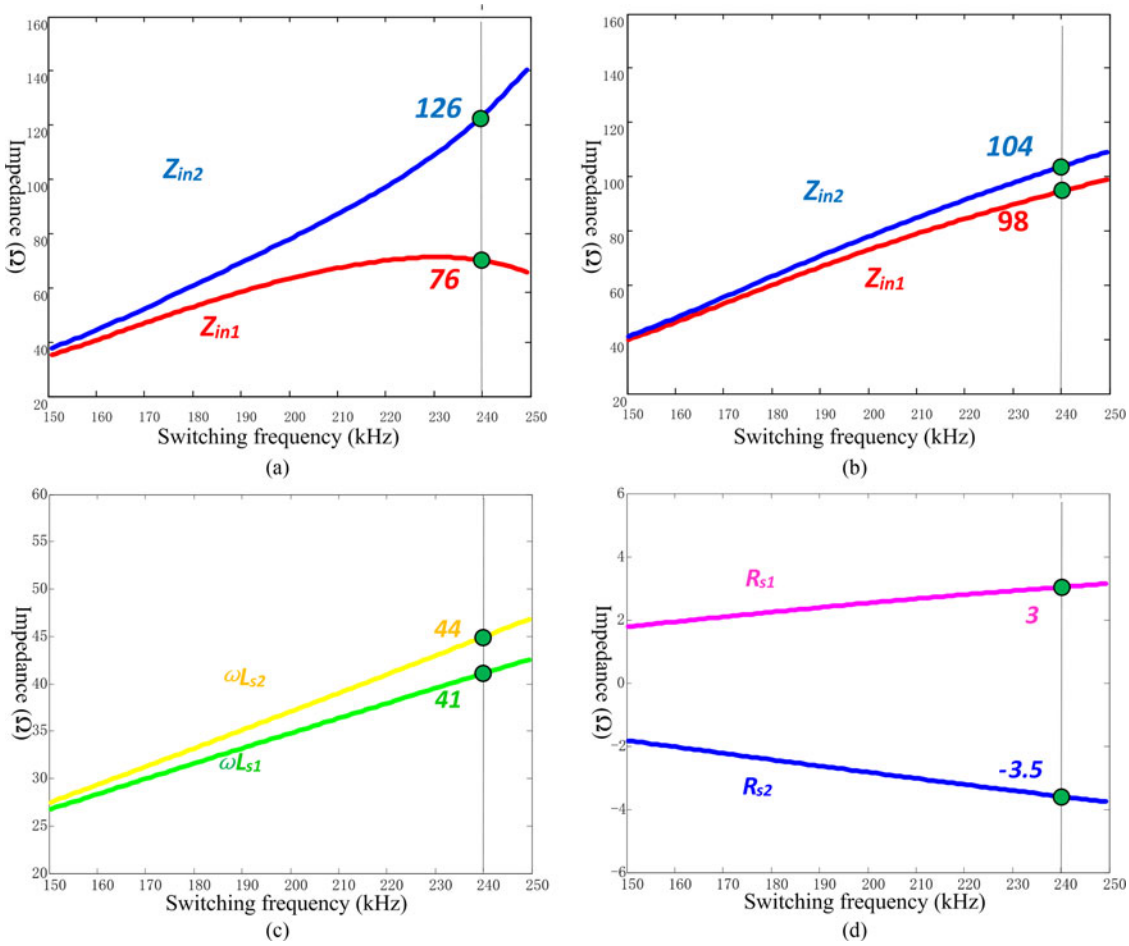

Fig. 11. Input impedance and virtual impedance under $L_{r2} = 1.05\ L_{r1}$, $C_{r2} = 0.95\ C_{r1}$, $L_{m2} = 1.05\ L_{m1}$, and $R_0 = 0.24\,\Omega$. (a) Input impedance of the conventional LLC. (b) Input impedance of the common-inductor LLC. (c) Virtual inductor of the common-inductor LLC. (d) Virtual resistor of the common-inductor LLC.

$1.05\ L_{s1}$, $C_{r2} = 0.95\ C_{r1}$, and $L_{m2} = 1.05\ L_{m1}$. Thus, there is almost the same current-sharing performance between the conventional two-phase LLC converter and the common-inductor two-phase LLC resonant converter if the virtual resistors are zero. A couple of virtual resistors of the common-inductor two-phase LLC converter are shown in Fig. 12(d): $R_{s1} = 0.1\,\Omega$ and $R_{s2} = -0.1\,\Omega$ at $f_s = 240$ kHz, which is very small and is a little influence of the input impedance.

As mentioned above, there is good current-sharing performance in this tolerance regardless of whether it is the conventional two-phase LLC converter or the common-inductor two-phase LLC converter. The virtual resistors and virtual inductors almost do not make a function.

Fig. 13 shows the comparison of the input impedance of the conventional two-phase LLC and the common-inductor two-phase LLC under $L_{r2} = 1.05\ L_{r1}$, $C_{r2} = 1.05\ C_{r1}$, $L_{m2} = 0.95\ L_{m1}$, and $R_o = 0.24\,\Omega$.

Fig. 13(a) and (b) shows $Z_{\text{in}1}$ and $Z_{\text{in}2}$ of the conventional two-phase LLC resonant converter and the common-inductor two-phase LLC resonant converter, respectively. Compared with the conventional two-phase LLC, the input impedance magnitude difference of two phases is reduced significantly based on the common-inductor two-phase LLC converter. For example, when $f_s = 240$ kHz, $Z_{\text{in}1} = 66\,\Omega$, and $Z_{\text{in}2} = 130\,\Omega$ for the conventional two-phase LLC converter, and $Z_{\text{in}1} = 96\,\Omega$ and $Z_{\text{in}2} = 102\,\Omega$ for the common-inductor two-phase LLC, the difference of each phase is reduced from 64 to 6 Ω.

Fig. 13(c) shows the virtual inductor of the common-inductor two-phase LLC resonant converter: $L_{s1} = 46\ \Omega$ and $L_{s2} = 44\ \Omega$ at $f_s = 240$ kHz. The virtual inductor tolerance is $L_{s2}/L_{s1} = 0.96$. Thus, the common-inductor two-phase LLC can almost be equivalent to the two-phase LLC converter under $L_{s2} = 0.96\ L_{s1}$, $C_{r2} = 1.05\ C_{r1}$, and $L_{m2} = 0.95\ L_{m1}$. There is conversely directional tolerance between the series inductor and the series capacitor. The input impedances between two phases are very close, as there are almost the same resonant frequencies.

A couple of virtual resistors of the common-inductor two-phase LLC converter are shown in Fig. 13(d): $R_{s1} = 0.1\,\Omega$ and $R_{s2} = -0.1\,\Omega$ at $f_s = 240$ kHz, which is very small and is a little influence of input impedance.

The above analysis shows that a couple of virtual resistors made a function to compensate the input impedance difference, as shown in Figs. 10 and 11. The virtual resistors and virtual

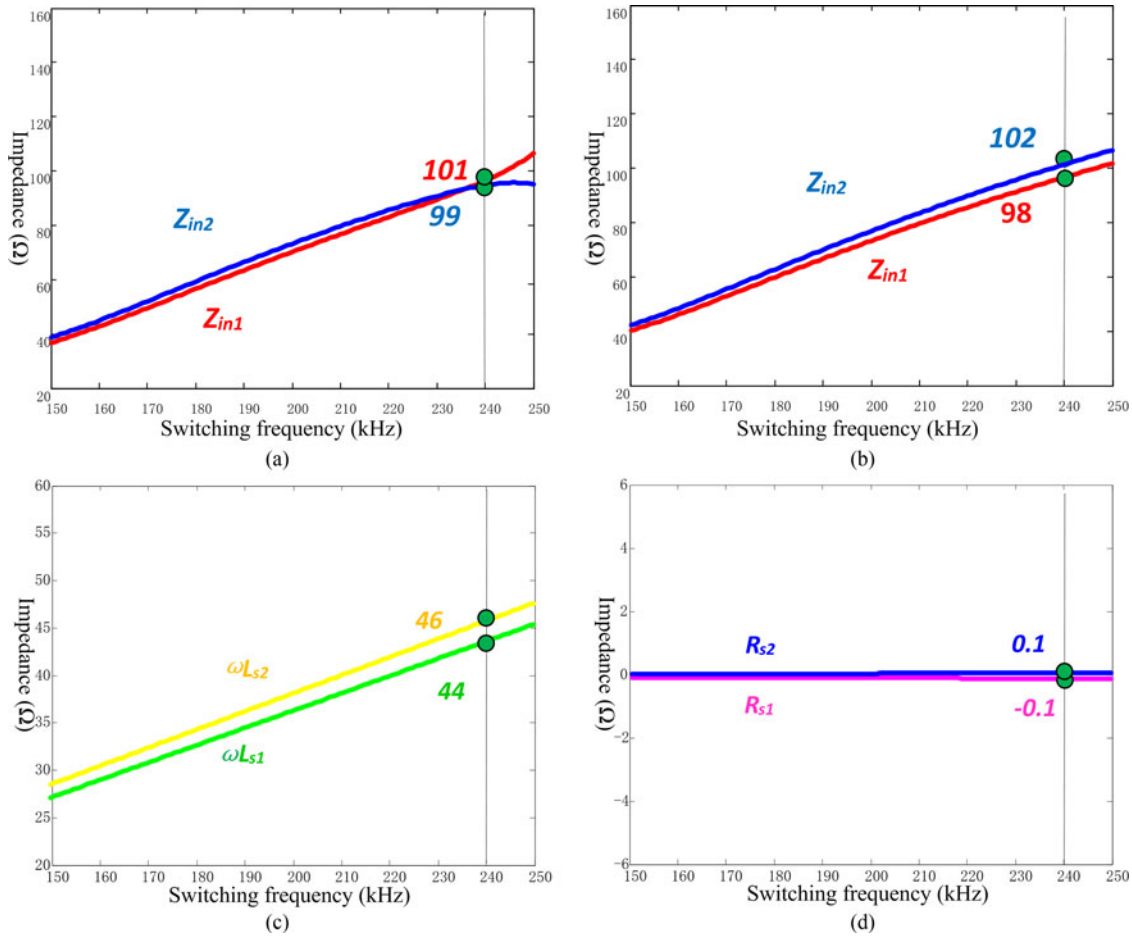

Fig. 12. Input impedance and virtual impedance under $L_{r2} = 1.05\ L_{r1}$, $C_{r2} = 1.05\ C_{r1}$, $L_{m2} = 1.05\ L_{m1}$, and $R_0 = 0.24\,\Omega$. (a) Input impedance of the conventional LLC. (b) Input impedance of the common-inductor LLC. (c) Virtual inductor of the common-inductor LLC. (d) Virtual resistor of the common-inductor LLC.

inductors almost do not function in Fig. 12, as the input impedance of each phase is almost the same in the conventional two-phase LLC converter. The virtual inductors play a role to compensate the input impedance difference of each phase in Fig. 13. Thus, there is input impedance matching owning to virtual resistor's function and virtual inductor's function in different component tolerances.

Next, the load current-sharing error of the common-inductor two-phase LLC resonant converter is calculated under different output loads.

Fig. 14 shows the load currents of two phases and the load current-sharing error under four corner cases: case 1 $L_{r2} = 1.05\ L_{r1}$, $C_{r2} = 1.05\ C_{r1}$, and $L_{m2} = 1.05\ L_{m1}$; case 2 $L_{r2} = 0.95\ L_{r1}$, $C_{r2} = 1.05\ C_{r1}$, and $L_{m2} = 1.05\ L_{m1}$; case 3 $L_{r2} = 1.05\ L_{r1}$, $C_{r2} = 1.05\ C_{r1}$, and $L_{m2} = 1.05\ L_{m1}$; case 4 $L_{r2} = 1.05\ L_{r1}$, $C_{r2} = 1.05\ C_{r1}$, and $L_{m2} = 0.95\ L_{m1}$.

The worst case for the common-inductor two-phase LLC resonant converter works under $L_{r2} = 1.05\ L_{r1}$, $C_{r2} = 0.95\ C_{r1}$, and $L_{m2} = 1.05\ L_{m1}$, as shown in Fig. 14(a). The load current-sharing error is 6% at the 50-A load current. The maximum current of phase 1 is 26.5 A, and the maximum current of phase 2 is 23.5 A, while the total load current is 50 A. However, it still achieves better current-sharing performance than the conventional two-phase LLC resonant converter in the same case.

IV. Extension of PIM

PIM technology is also applicable to many resonant converters. The above-mentioned common-inductor two-phase LLC resonant converter is just one example. Section IV-A introduces the common-capacitor two-phase LLC resonant converter as another embodiment, in which the resonant capacitors of two phases are connected in parallel to construct the virtual impedance. In Section IV-B, the method of constructing the virtual impedance based on common inductor or common capacitor is extended to multiphase (i.e., more than two phases) applications. In Section IV-C, PIM technology is extended to other types of resonant converters, such as CLL resonant converters, SRCs, LCC converters, and so on.

A. Common-Capacitor Two-Phase LLC Resonant Converter

Two LLC converters are connected in parallel and connect the resonant capacitor in parallel, as shown in Fig. 15. By connecting two resonant capacitors in parallel, the operation of two resonant

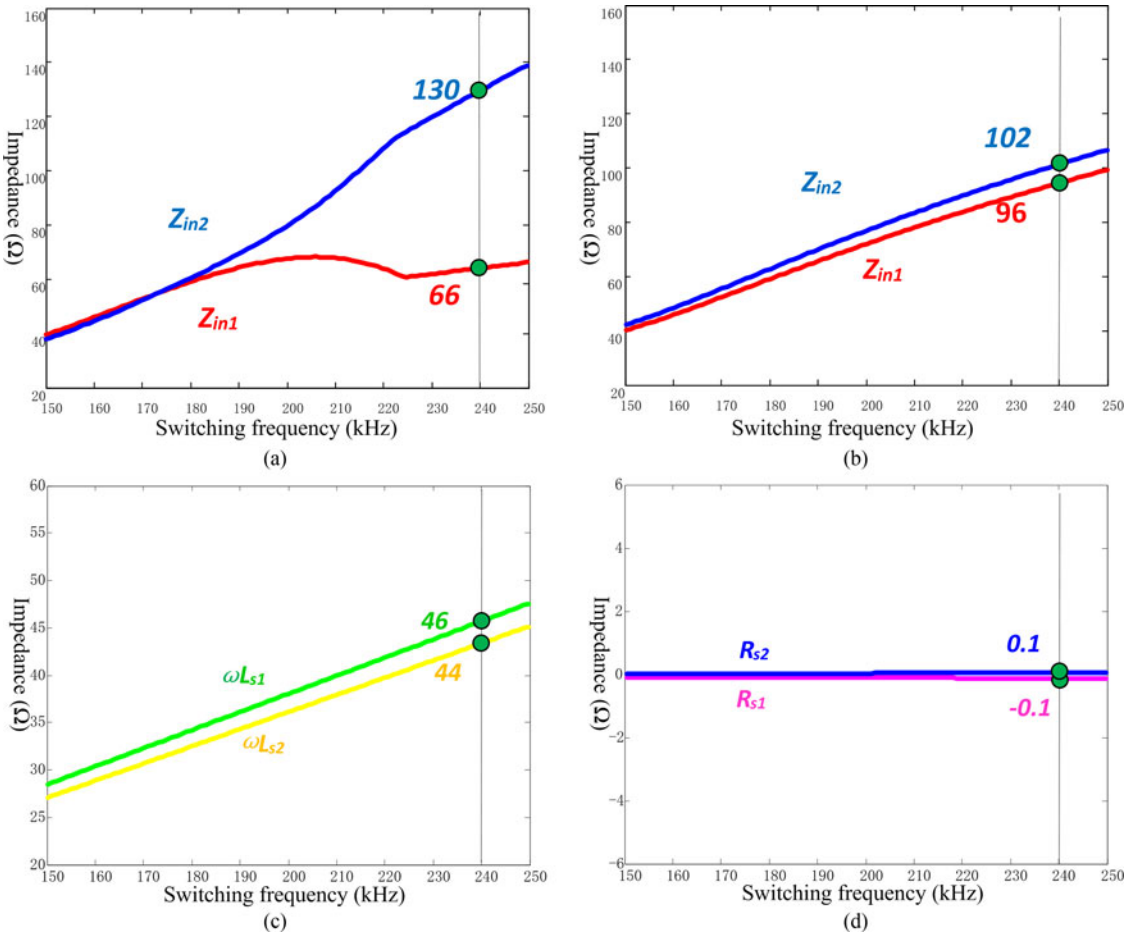

Fig. 13. Input impedance and virtual impedance under $L_{r2} = 1.05\ L_{r1}$, $C_{r2} = 1.05\ C_{r1}$, $L_{m2} = 0.95\ L_{m1}$, and $R_0 = 0.24\,\Omega$. (a) Input impedance of the conventional LLC. (b) Input impedance of the common-inductor LLC. (c) Virtual inductor of the common-inductor LLC. (d) Virtual resistor of the common-inductor LLC.

tanks is coupled. This section will decouple the operation of these two phases and illustrate how the common-capacitor connection can improve the current-sharing performance.

Fig. 16 shows the transformation from a single capacitor to two branches. The equivalent circuit of the two-phase common-inductor LLC converter is shown in Fig. 16(a), where I_{Lr1} and I_{Lr2} is the resonant current through phases 1 and 2, respectively, C_s is the combination of two resonant capacitors C_{r1} and C_{r2}), V_s is the voltage across C_s, and I_s is the current through C_s. The total resonant capacitance C_s is shown as

$$C_s = C_{r1} + C_{r2}. \tag{25}$$

Based on the circuit theory [33], the circuit shown in Fig. 16(a) can be expressed equivalently, as shown in Fig. 16(b). The single capacitor C_s is split into two impedances (Z_{s1} and Z_{s2}). The current I_{Lr1} flows through Z_{s1} and I_{Lr2} flows through Z_{s2}. The voltages at points A_1 and A_2 are the same.

The impedances of Z_{s1} and Z_{s2} can be expressed as

$$\begin{cases} Z_{s1} = R_{s1} + {}^{1}/_{sC_{s1}} \\ Z_{s2} = R_{s2} + {}^{1}/_{sC_{s2}}. \end{cases} \tag{26}$$

Thus, the single capacitor is expressed as

$$\frac{\left(R_{s1} + {}^{1}/_{sC_{s1}}\right)\left(R_{s2} + {}^{1}/_{sC_{s2}}\right)}{(R_{s1} + R_{s2}) + \left({}^{1}/_{sC_{s1}} + {}^{1}/_{sC_{s2}}\right)} = {}^{1}/_{sC_s}. \tag{27}$$

Therefore, one capacitor (*Cs*) has been separated into two branches: R_{s1}, C_{s1} and R_{s2}, C_{s2}. The current through each branch is the same as the original current, I_{Lr1} and I_{Lr2}.

Therefore, the phasor diagram for I_s, I_{Lr1}, and I_{Lr2} can be shown in Fig. 17, where the phase of I_s is used as the reference. It notes that I_{Lr1} and I_{Lr2}, I_{Lr1} leads I_s and I_{Lr2} lags I_s.

The voltage V_s is also calculated by equivalent impedances as

$$V_s = I_{Lr1} * R_{s1} + {}^{I_{Lr1}}/_{j\omega C_{s1}} \tag{28}$$

$$V_s = I_{Lr2} * R_{s2} + {}^{I_{Lr2}}/_{j\omega C_{s2}}. \tag{29}$$

The phase diagrams for (22) and (23) are shown in Fig. 18(a) and (b), respectively.

The phasor diagram shown in Fig. 18(a) shows that R_{s1} is a negative value. It should be emphasized that the phasor diagram shown in Fig. 18(b) indicates that R_{s2} must be a positive value

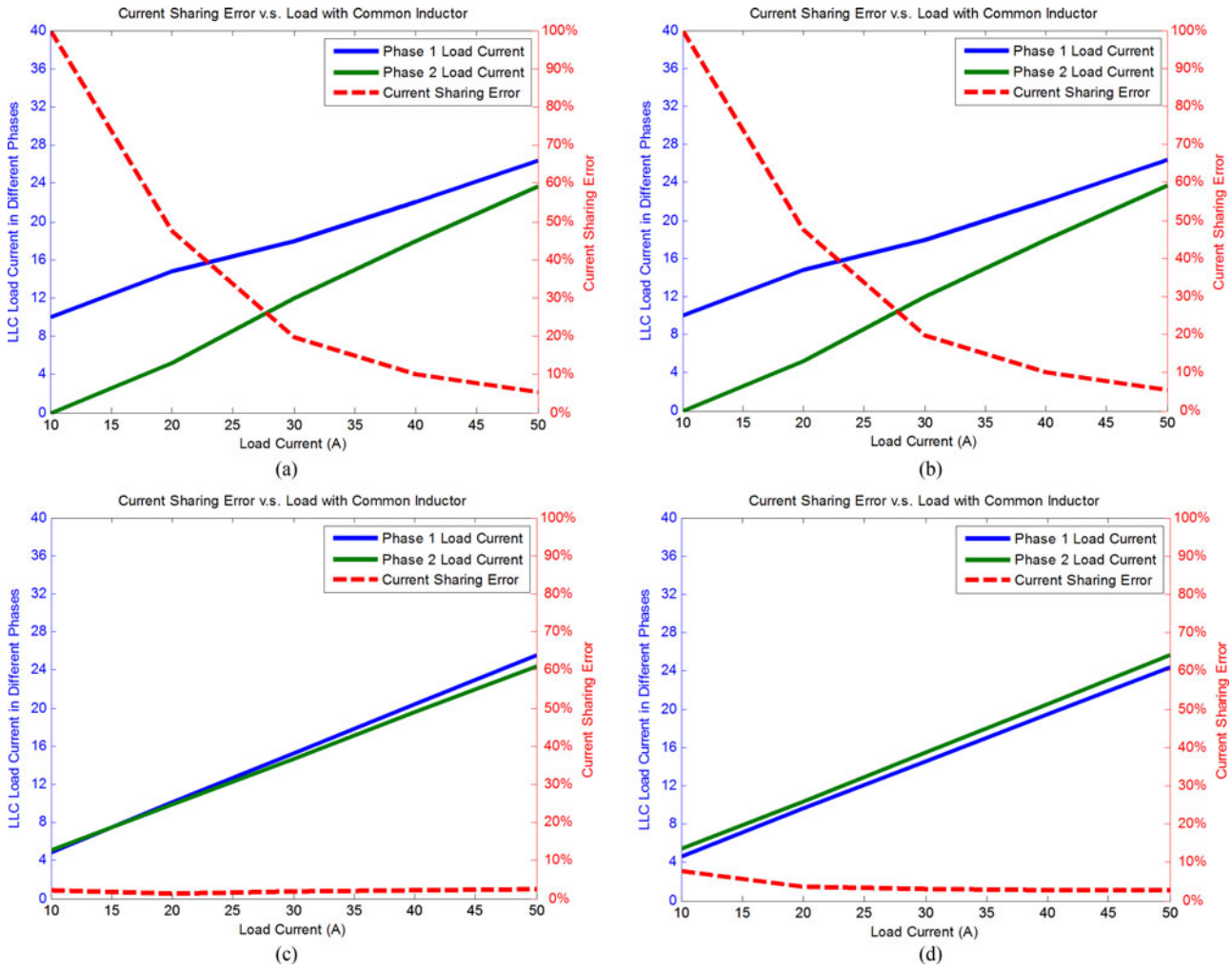

Fig. 14. Load current-sharing error of the common-inductor two-phase LLC resonant converter. (a) $L_{r2} = 1.05\ L_{r1}$, $C_{r2} = 1.05\ C_{r1}$, and $L_{m2} = 1.05\ L_{m1}$. (b) $L_{r2} = 0.95\ L_{r1}$, $C_{r2} = 1.05\ C_{r1}$, and $L_{m2} = 1.05\ L_{m1}$. (c) $L_{r2} = 1.05\ L_{r1}$, $C_{r2} = 0.95\ C_{r1}$, and $L_{m2} = 1.05\ L_{m1}$. (d) $L_{r2} = 1.05\ L_{r1}$, $C_{r2} = 1.05\ C_{r1}$, and $L_{m2} = 0.95\ L_{m1}$.

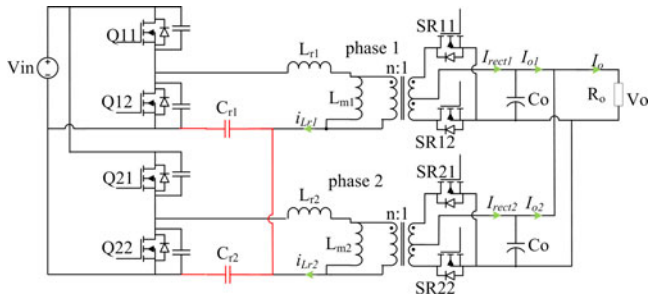

Fig. 15. Common-capacitor two-phase LLC resonant converter.

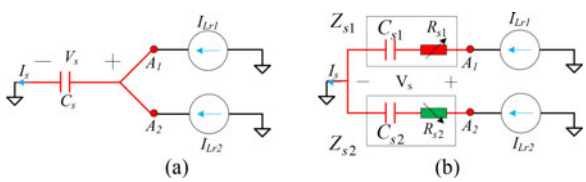

Fig. 16. Transformation from a single capacitor to two branches. (a) Common capacitor. (b) Equivalent circuit.

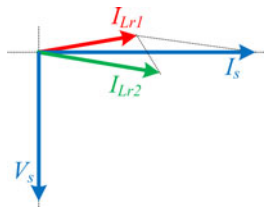

Fig. 17. Phase diagram of I_s, I_{Lr1}, and I_{Lr2}.

in order to satisfy (4). This is due to the fact that the phase angle between V_s and I_{Lr2} is smaller than 90°.

The impact of this coupling is equivalent to two components in each phase: a virtual resistor and an equivalent inductor connected in series, as shown in Fig. 19.

More importantly and more helpfully, a positive virtual resistor is added to the phase, which would generate higher current (phase 2 in this case) to reduce the actual resonant current. A negative virtual resistor is added to the phase, which would generate less resonant current (phase 1 in this case). The end result is that the current in two phases is more balanced. They change

Fig. 18. (a) Phase diagram of V_s, I_s, and I_{Lr1}. (b) Phase diagram of V_s, I_s, and I_{Lr1}.

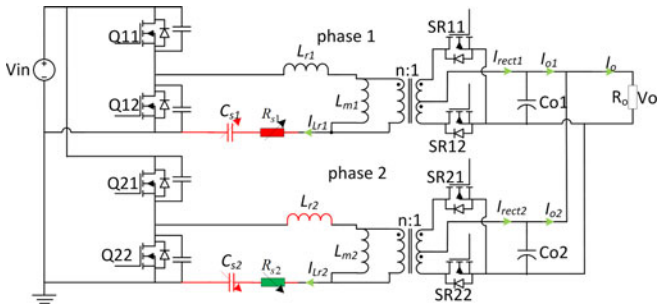

Fig. 19. Decoupled equivalent circuit of the common-inductor LLC converter.

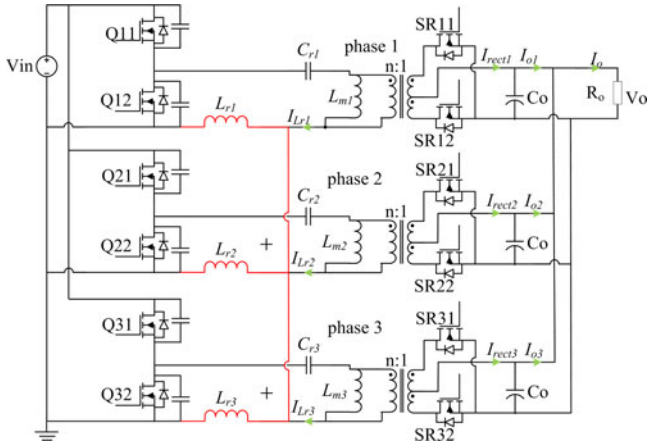

Fig. 20. Common-inductor three-phase LLC resonant converter.

the equivalent impedance of the resonant tank so that current sharing can be achieved.

B. Common-Inductor or Common-Capacitor Multiphase LLC Resonant Converter

To extend the PIM to multiphase (i.e., more than two phases) applications, Fig. 20 shows a common-inductor three-phase LLC resonant converter. The resonant inductor of each phase is connected in parallel. The operation of three resonant tanks is coupled. This section will decouple the operation of these three phases.

Fig. 21 shows the transformation from a single inductor to three branches. The equivalent circuit of the three-phase common-inductor LLC converter is shown in Fig. 21(a), where I_{Lr1}, I_{Lr2}, and I_{Lr3} are the resonant currents through phases 1-3, respectively, L_s is the combination of three resonant inductors L_{r1}, L_{r2}, and L_{r3}), V_s is the voltage across L_s, and I_s is the current through L_s.

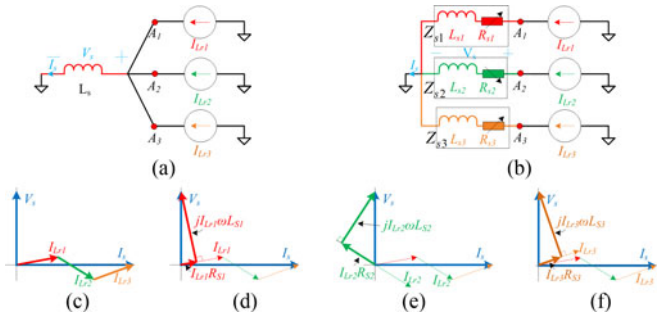

Fig. 21. Transformation from a single inductor to three branches. (a) Common inductor. (b) Equivalent circuit. (c) Phase diagram of V_s and I_{Lr1}. (d) Phase diagram of V_s and I_{Lr1}. (e) Phase diagram of V_s and I_{Lr1}. (f) Phase diagram of V_s and I_{Lr3}.

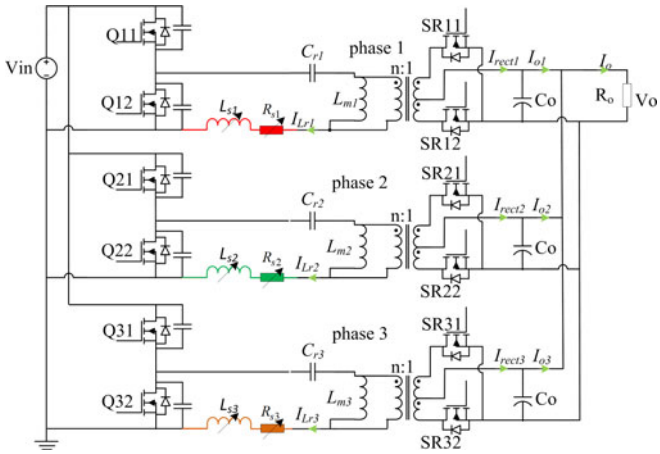

Fig. 22. Equivalent common-inductor three-phase LLC resonant converter.

The current I_s is expressed as

$$I_s = I_{Lr1} + I_{Lr2} + I_{Lr3}. \tag{30}$$

Based on the circuit theory [33], the circuit shown in Fig. 21(a) can be expressed equivalently, as shown in Fig. 21(b). The single inductor L_s is split into three impedances (Z_{s1}, Z_{s2}, and Z_{s3}). The current I_{Lr1} flows through Z_{s1}, I_{Lr2} flows through Z_{s2}, and I_{Lr3} flows through Z_{s3}. The voltages at points A_1, A_2, and A_3 are same.

It is noted that although there are several possibilities about three resonant phases, there is always several resonant current lead reference current and the other resonant current lag reference current from (23). One operation about the phasor diagram for I_s, I_{Lr1}, I_{Lr2}, and I_{Lr3} is shown in Fig. 21(c), where the phase of I_s is used as the reference. I_{Lr1} and I_{Lr3} lead I_s and I_{Lr2} lags I_s. The phasor diagram, as shown in Fig. 21(d) and (f), shows that R_{s1} and R_{s3} is a positive value. It should be emphasized that the phasor diagram shown in Fig. 21(e) indicates that R_{s2} must be a negative value in order to satisfy (23).

This is due to the fact that the phase angle between V_s and I_{Lr2} is larger than 90°. The equivalent decoupled common-capacitor three-phase LLC resonant converter is shown in Fig. 22.

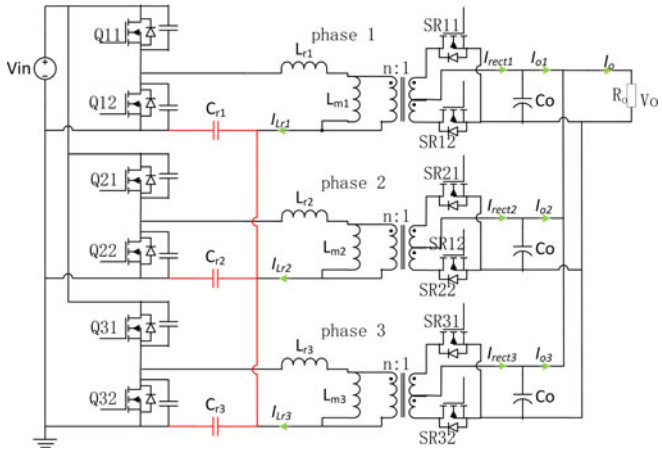

Fig. 23. Common-capacitor three-phase LLC resonant converter.

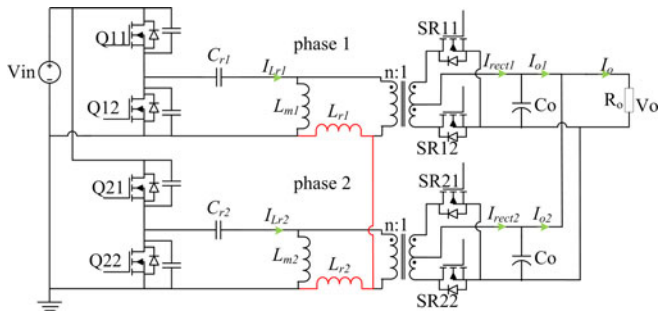

Fig. 24. Common-inductor two-phase CLL resonant converter.

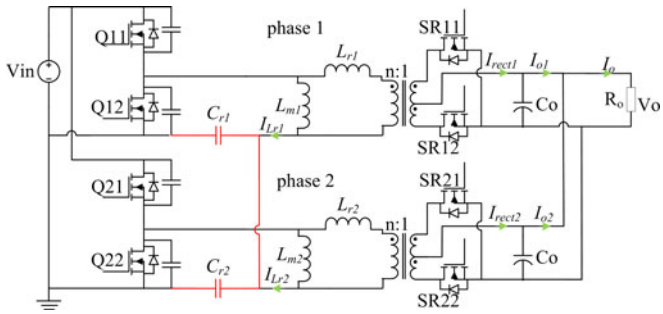

Fig. 25. Common-capacitor two-phase CLL resonant converter.

The common-capacitor three-phase LLC resonant converter is shown in Fig. 23.

C. Other Resonant Converter Under PIM Technology

A CLL resonant converter has been proposed [35]–[40], and it has a similar performance as the traditional LLC converter. From the viewpoint of PIM technology, a common-inductor two-phase CLL resonant converter is built and shown in Fig. 24.

Two inductors are connected in parallel. The virtual impedance can be achieved by "virtual open." Similarly, a common-capacitor two-phase CLL resonant converter is shown in Fig. 25.

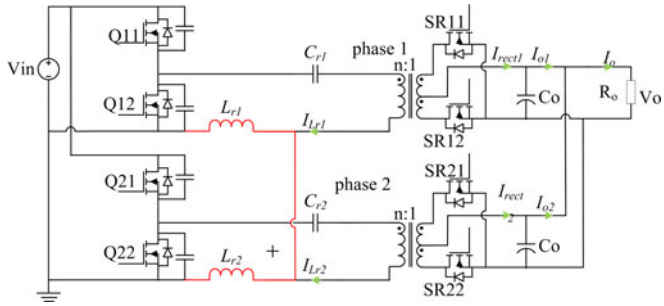

Fig. 26. Common-inductor two-phase SRC.

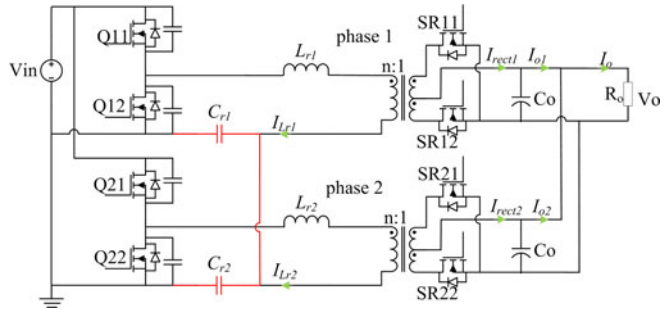

Fig. 27. Common-capacitor two-phase SRC.

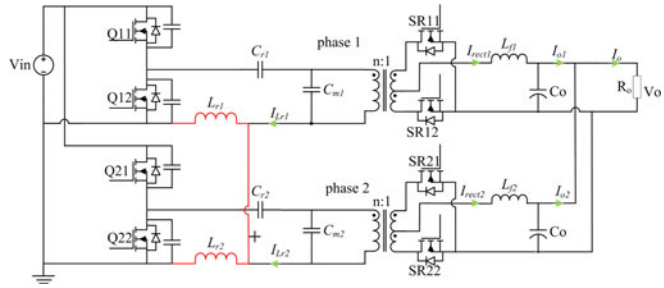

Fig. 28. Common-inductor two-phase LCC resonant converter.

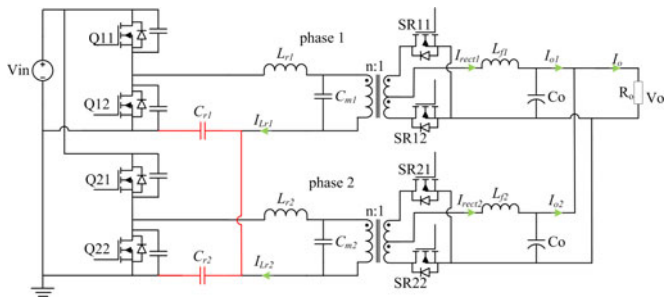

Fig. 29. Common-capacitor two-phase LCC resonant converter.

From the viewpoint of PIM technology, it is also to construct virtual impedance based on the SRC. A common-inductor two-phase SRC is shown in Fig. 26. A common-capacitor two-phase SRC is shown in Fig. 27.

From the viewpoint of PIM technology, it is also to construct virtual impedance based on the LCC resonant converter. A common-inductor two-phase LCC resonant converter is shown in Fig. 28. Similarly, a common-inductor two-phase LCC resonant converter is shown in Fig. 29.

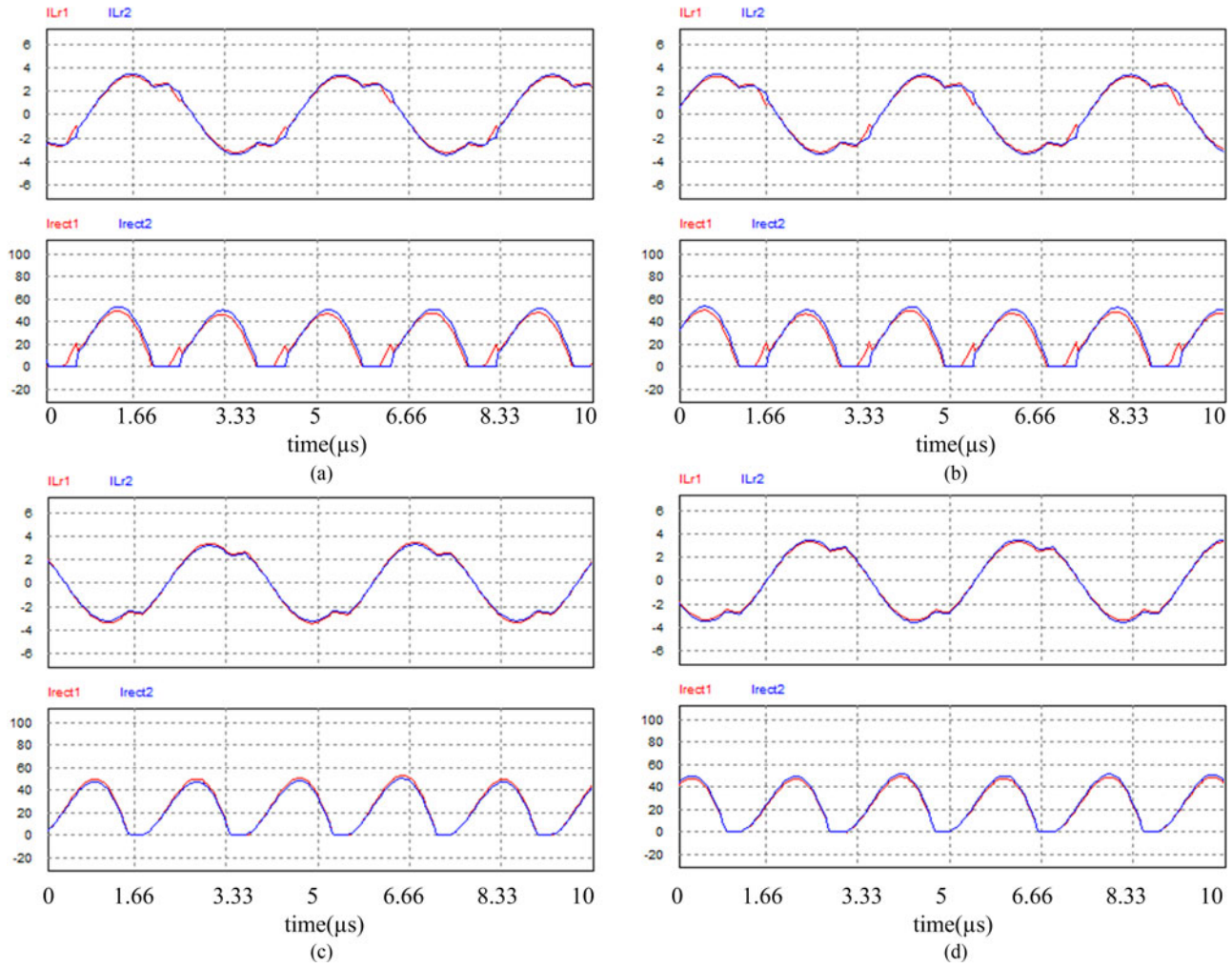

Fig. 30. Simulation results of the conventional two-phase LLC converter with +5% tolerance at the 400-V input condition. (a) $L_{r2} = 1.05\ L_{r1}$, $C_{r2} = 1.05\ C_{r1}$, and $L_{m2} = 1.05\ L_{m1}$. (b) $L_{r2} = 0.95\ L_{r1}$, $C_{r2} = 1.05\ C_{r1}$, and $L_{m2} = 1.05\ L_{m1}$. (c) $L_{r2} = 1.05\ L_{r1}$, $C_{r2} = 0.95\ C_{r1}$, and $L_{m2} = 1.05\ L_{m1}$. (d) $L_{r2} = 1.05\ L_{r1}$, $C_{r2} = 1.05\ C_{r1}$, and $L_{m2} = 0.95\ L_{m1}$.

V. Simulation Results

Furthermore, to verify and compare the current-sharing performance, in this section, PSIM simulation results of the common-inductor LLC resonant converter will be provided. Four types of tolerance combination will be included: (a) $L_{r2} = 1.05\ L_{r1}$, $C_{r2} = 1.05\ C_{r1}$, and $L_{m2} = 1.05\ L_{m1}$; (b) $L_{r2} = 0.95\ L_{r1}$, $C_{r2} = 1.05\ C_{r1}$, and $L_{m2} = 1.05\ L_{m1}$; (c) $L_{r2} = 1.05\ L_{r1}$, $C_{r2} = 0.95\ C_{r1}$, and $L_{m2} = 1.05\ L_{m1}$; and (d) $L_{r2} = 1.05\ L_{r1}$, $C_{r2} = 1.05\ C_{r1}$, and $L_{m2} = 0.95\ L_{m1}$.

The simulation is conducted under 400-V input and total 50-A load condition. The rated output voltage is 12 V. The parameters of two phases are shown in Table II.

Fig. 30 shows the PSIM simulation waveforms of the resonant current and the rectifier current of the common-inductor two-phase LLC resonant converter.

In Fig. 30(a) and (b), when the tolerance on C_r (b) and the tolerance on L_m (c) deviate in the same direction, the two-phase current is almost identical, which verifies the FHA calculation results in Fig. 30(a) and (b). Also, good current-sharing performance is achieved when the tolerance on C_r (b) and the tolerance on L_m (c) deviate in the opposite direction shown in Fig. 30(c) and (d).

TABLE II
Parameters of the Two-Phase LLC Converter in PSIM

	Resonant Inductor L_r	Resonant capacitor C_r	Magnetizing inductor L_m
Phase 1 (reference)	29 μH	12 nF	95 μH
Phase 2 (a)	30.5 μH (+5%)	12.6 nF (+5%)	100 μH (+5%)
Phase 2 (b)	28.5 μH (−5%)	12.6 nF (+5%)	100 μH (+5%)
Phase 2 (c)	30.5 μH (+5%)	11.4 nF (−5%)	100 μH (+5%)
Phase 2 (d)	30.5 μH (+5%)	12.6 nF (+5%)	90 μH (−5%)

Table III shows the load current data comparison of the common-inductor two-phase LLC resonant converter. The load current error (σ_{load}) between the two phases is only 2%. It is verified that good current-sharing performance can be achieved under the PIM method.

Considering the leakage inductance of the transformer, the parameters and tolerances based on the experimental prototype

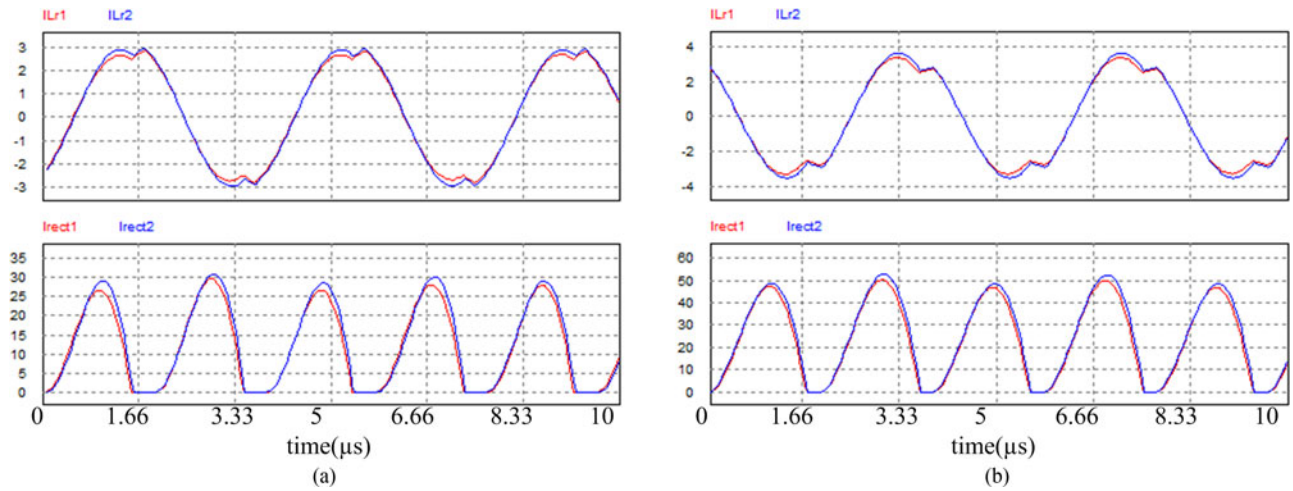

Fig. 31. Simulation for the common-inductor two-phase LLC converter at (a) 25-A load and (b) 50-A load.

TABLE III
DATA COMPARISON OF SIMULATION OF THE COMMON-INDUCTOR LLC RESONANT CONVERTER

Tolerances	Common-inductor two-phase LLC		
	$I_{\mathrm{rect1\_ave}}$	$I_{\mathrm{rect2\_ave}}$	$\sigma_{\mathrm{load\_PSIM}}$
Type #1 (a, b, c) = (1.05, 1.05, 1.05)	24.5	25.5	2%
Type #2 (a, b, c) = (0.95, 1.05, 1.05)	24.5	25.5	2%
Type #3 (a, b, c) = (1.05, 0.95, 1.05)	25.5	24.5	2%
Type #4 (a, b, c) = (1.05, 1.05, 0.95)	24.2	25.8	1.6%

TABLE IV
EXPERIMENTAL PROTOTYPE PARAMETERS

	Resonant Inductor L_{r}	Resonant capacitor C_{r}	Magnetizing inductor L_{m}	Leakage Inductance L_{e}
Phase 1	22.5 μH	12.3 nF	95 μH	6 μH(∼21% of total $L_{\mathrm{r}1}$)
Phase 2	24.5 μH (+8.9%)	12.7 nF (+3.3%)	92 μH (-3.2%)	6.5 μH (+8.3%)

TABLE V
CURRENT-SHARING ERROR AT EXPERIMENTAL PARAMETER TOLERANCE

Total current	Phase	Common-inductor two-phase LLC			
		$I_{\mathrm{Lr\_rms}}$	$\sigma_{\mathrm{resonant}}$	$I_{\mathrm{rect\_ave}}$	σ_{load}
25 A	Phase 1	2.2 A	2.2%	12.1 A	3.2%
	Phase 2	2.3 A		12.9 A	
50 A	Phase 1	2.4 A	2%	24.3 A	2.8%
	Phase 2	2.6 A		25.7 A	

TABLE VI
PROTOTYPE SPECIFICATIONS

Switching frequency	180–270 kHz
Input Voltage	340–400 V
Output Voltage	12 V
Output Power	300 W × 2
Transformer Ratio n	20:1
Output Capacitance	1790 μF
Series Capacitance (C_{r})	12.3 nF (Phase1) 12.7 nF (Phase2)
Resonant Inductance (L_{r})	22.5 μH (Phase1) 24.5 μH (Phase2)
Leakage Inductance (L_{e})	6 μH (Phase1) 6.5 μH (Phase2)
Magnetizing Inductance (L_{m})	95 μH (Phase1) 92 μH (Phase2)
Output Capacitance	1790 μF (100 μF × 8 + 330 μF × 3)
Half-bridge MOSFET	IPB60R190C6
SR MOSFET	BSC011N03LS

are shown in Table IV. It is the worst case as the tolerance directions on L_r and L_m are opposite. The leakage inductor of the transformer is now taken into consideration. The design total power is 600 W (300 W × 2).

Fig. 31 shows the simulation waveforms of the common-inductor two-phase LLC resonant converter when the total load current is 25 and 50 A repetitively. A common-inductor two-phase LLC converter could achieve significantly improved load current sharing.

Table V shows the resonant current-sharing error $\sigma_{\mathrm{resonant}}$ and the load current-sharing error σ_{load} based on the prototype parameters and tolerances of the conventional two-phase LLC converter and the common-inductor two-phase LLC converter under the total load current of 25 and 50 A.

It is observed that the resonant current-sharing error is low (such as smaller than 5%); the load current-sharing error becomes very reasonable. Thus, it is believed that good resonant current sharing guarantees good load current sharing at heavy load.

VI. EXPERIMENTAL RESUITS

A 600-W common-inductor two-phase LLC resonant converter prototype is built to verify the feasibility and to demonstrate the advantages of the PIM method. The resonant tank parameters for the single-phase converter are designed based on the traditional design method [34]. The design method of the proposed multiphase LLC resonant converter is the same as that of the single-phase LLC converter.

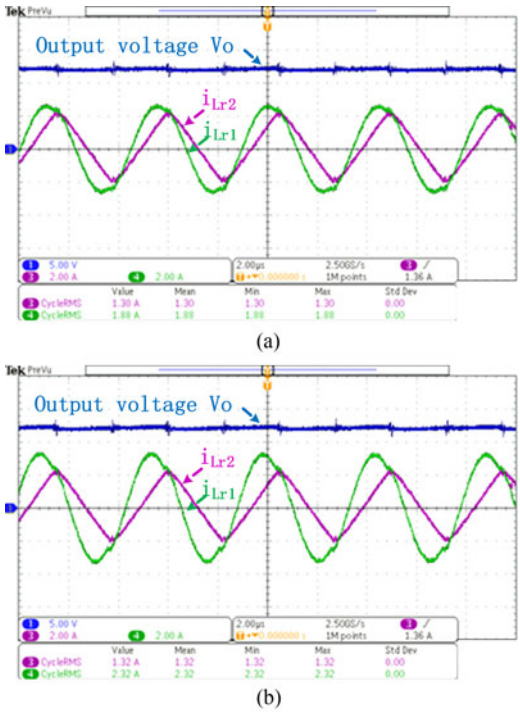

Fig. 32. Experimental waveforms of the conventional two-phase LLC converter. (a) Steady state at 15-A load. (b) Steady state at 25-A load. Ch1: output voltage; Ch3: resonant current of phase 2; Ch4: resonant current of phase 1.

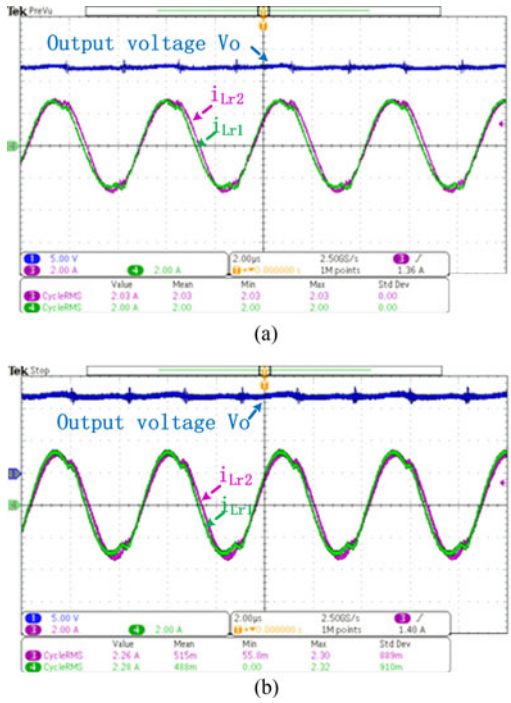

Fig. 33. Experimental waveforms of the common-inductor LLC converter. (a) Steady state at 15-A load. (b) Steady state at 25-A load. (c) Steady state at 50-A load. Ch1: output voltage; Ch3: resonant current of phase 2; Ch4: resonant current of phase 1.

In the experimental prototype, the current on the secondary side is 50 A (very high), and the printed-circuit-board track has been made as short as possible to reduce the parasitic inductance. Thus, it is not possible to measure the load current of each phase directly. From PSIM simulation results, good resonant current sharing means good load current sharing. Resonant currents are measured as current-sharing performance evaluation. The prototype parameters are shown in Table VI.

Fig. 32 shows the experimental waveforms of the conventional two-phase LLC converter at the total load current of 15 and 25 A. The switching frequency is 245 kHz in Fig. 32(a) and 240 kHz in Fig. 32(b).

Fig. 33 shows the experimental waveforms of the proposed common-inductor two-phase LLC resonant converter. The resonant current i_{Lr2} is of almost triangular waveform, which means that phase 2 does not provide the power for the output load in Fig. 33(a) and (b).

The resonant current i_{Lr1} is almost the same as i_{Lr2} at 25- and 50-A load. A very small angle difference between them is shown at different loads. To show the current-sharing performance, the resonant current and resonant current-sharing error are shown in Fig. 34 for both the conventional and the proposed converters.

As shown in Fig. 34(a), the resonant current-sharing error increases from 10% to 28% for load current of 5–25 A for the conventional two-phase LLC converter. The resonant current-sharing error is reduced from 6.3% to 0.44% for the proposed converter when load current changes from 5 to 50 A in Fig. 34(b). Thus, the resonant current-sharing error can be significantly reduced by using the proposed method.

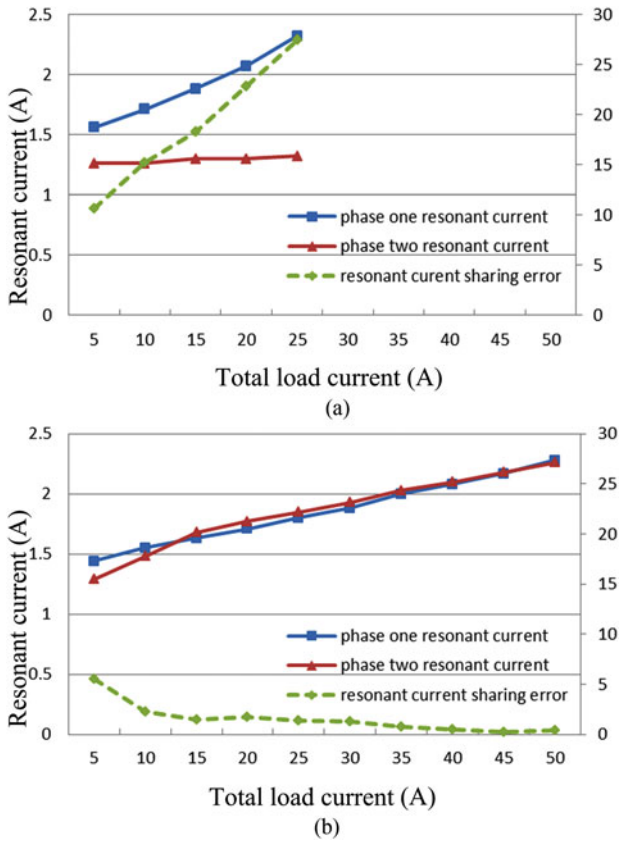

Fig. 34. Resonant current of (a) the conventional two-phase LLC resonant converter and (b) the common-inductor two-phase LLC resonant converter.

VII. Conclusion

A PIM technology is proposed in this paper to achieve load sharing automatically for multiphase resonant converters. The PIM technology views the impedance network as passive components in addition to virtual positive resistors and negative resistors. A common-inductor two-phase LLC resonant converter is analyzed as one example, in which the resonant inductors in two phases are connected in parallel. No additional components are needed to achieve current sharing. The analysis results show that the input impedances of each phase are more balanced under virtual positive and negative resistor's function. Thus, the current-sharing error is significantly reduced in the common-inductor two-phase LLC resonant converter. Many new topologies based on PIM technology are derived, such as the common-capacitor two-phase LLC resonant converter, the three-phase LLC resonant converter, the common-inductor/capacitor two-phase SRC, the common-inductor/capacitor two-phase CLL resonant converter, the common-inductor/capacitor LCC resonant converter, and the common-inductor/capacitor multiphase resonant converter. A 600-W common-inductor two-phase LLC resonant converter prototype is built to verify the feasibility and demonstrate the advantages of the proposed method. The experimental results show that the resonant current-sharing error reduces 63 times and is only 0.44% at the 600-W total load power. The analysis, simulation, and experimental results have verified the feasibility and demonstrated advantages of PIM technology.

References

[1] B. Yang, "Topology investigation for front end DC/DC power conversion for distributed power system," Ph.D. dissertation, Dept. Elect. Comput. Eng., Virginia Polytech. Inst. State Univ., Blacksburg, VA, USA, 2003.

[2] Y. Zhang, D. Xu, M. Chen, Y. Han, and Z. Du, "LLC resonant converter for 48 V to 0.9 V VRM," in *Proc. IEEE 35th Annu. Power Electron. Spec. Conf.*, 2004, vol. 3, pp. 1848–1854.

[3] Y. Zhang, D. Xu, M. Chen, Y. Han, and Z. Du, "LLC resonant converter for 48 V to 0.9 V VRM," in *Proc. Power Electron. Spec. Conf.*, 2004, vol. 3, pp. 1848–1854.

[4] B. Lu, W. Liu, Y. Liang, F. C. Lee, and J. D. Van Wyk, "Optimal design methodology for LLC resonant converter," in *Proc. 21st Annu. IEEE Appl. Power Electron. Conf. Expo.*, 2006, p. 6.

[5] S. De Simone, C. Adragna, C. Spini, and G. Gattavari, "Design-oriented steady-state analysis of LLC resonant converters based on FHA," in *Proc. Int. Symp. Power Electron., Elect. Drives, Autom., Motion*, 2006, pp. 200–207.

[6] H.-S. Choi, "Design consideration of half-bridge LLC resonant converter," *J. Power Electron.*, vol. 7, pp. 13–20, 2007.

[7] D. Fu, B. Lu, and F. C. Lee, "1 MHz high efficiency LLC resonant converters with synchronous rectifier," in *Proc. Power Electron. Spec. Conf.*, 2007, pp. 2404–2410.

[8] J. Jee-Hoon and K. Joong-Gi, "Theoretical analysis and optimal design of LLC resonant converter," in *Proc. Eur. Conf. Power Electron. Appl.*, 2007, pp. 1–10.

[9] C. Adragna, S. De Simone, and C. Spini, "A design methodology for LLC resonant converters based on inspection of resonant tank currents," in *Proc. Appl. Power Electron. Conf. Expo.*, 2008, pp. 1361–1367.

[10] K. Bong-Chul, P. Ki-Bum, K. Chong-Eun, L. Byoung-Hee, and M. Gun-Woo, "LLC resonant converter with adaptive link-voltage variation for a high-power-density adapter," *IEEE Trans. Power Electron.*, vol. 25, no. 9, pp. 2248–2252, Sep. 2010.

[11] P. Drgona, M. Frivaldsky, and A. Prikopova, "Optimal design of digital control system for LLC resonant converter," in *Proc. Int. Conf. Appl. Electron.*, 2010, pp. 1–4.

[12] D. Fu, F. C. Lee, and W. Shuo, "Investigation on transformer design of high frequency high efficiency dc-dc converters," in *Proc. Appl. Power Electron. Conf. Expo.*, 2010, pp. 940–947.

[13] C. Oeder, A. Bucher, J. Stahl, and T. Duerbaum, "A comparison of different design methods for the multiresonant LLC converter with capacitive output filter," in *Proc. 12th Workshop Control Model. Power Electron.*, 2010, pp. 1–7.

[14] G. Ivensky, S. Bronshtein, and A. Abramovitz, "Approximate analysis of resonant LLC DC-DC converter," *IEEE Trans. Power Electron.*, vol. 26, no. 11, pp. 3274–3284, Nov. 2011.

[15] X. Fang, H. Hu, J. Shen, and I. Batarseh, "An optimal design of the LLC resonant converter based on peak gain estimation," in *Proc. Appl. Power Electron. Conf. Expo.*, 2012, pp. 1286–1291.

[16] M. T. Zhang, M. M. Jovanovic, and F. C. Y. Lee, "Analysis and evaluation of interleaving techniques in forward converters," *IEEE Trans. Power Electron.*, vol. 13, no. 4, pp. 690–698, Jul. 1998.

[17] R. Hermann, S. Bernet, S. Yongsug, and P. K. Steimer, "Parallel connection of integrated gate commutated thyristors (IGCTs) and diodes," *IEEE Trans. Power Electron.*, vol. 24, no. 9, pp. 2159–2170, Sep. 2009.

[18] J. Rabkowski, D. Peftitsis, and H. P. Nee, "Parallel-operation of discrete SiC BJTs in a 6-kW/250-kHz DC/DC boost converter," *IEEE Trans. Power Electron.*, vol. 29, no. 5, pp. 2482–2491, May 2014.

[19] Z. Hu, Y. Qiu, L. Wang, and Y.-F. Liu, "An interleaved LLC resonant converter operating at constant switching frequency," *IEEE Trans. Power Electron.*, vol. 29, no. 6, pp. 2931–2943, Jun. 2014.

[20] H. Figge, T. Grote, N. Froehleke, J. Boecker, and P. Ide, "Paralleling of LLC resonant converters using frequency controlled current balancing," in *Proc. IEEE Power Electron. Spec. Conf.*, 2008, pp. 1080–1085.

[21] K. Bong-Chul, P. Ki-Bum, and M. Gun-Woo, "Analysis and design of two-phase interleaved LLC resonant converter considering load sharing," in *Proc. IEEE Energy Convers. Congr. Expo.*, 2009, pp. 1141–1144.

[22] E. Orietti, P. Mattavelli, G. Spiazzi, C. Adragna, and G. Gattavari, "Current sharing in three-phase LLC interleaved resonant converter," in *Proc. IEEE Energy Convers. Congr. Expo.*, 2009, pp. 1145–1152.

[23] Z. Hu, Y. Qiu, L. Wang, and Y.-F. Liu, "An interleaved LLC resonant converter operating at constant switching frequency," in *Proc. IEEE Energy Convers. Congr. Expo.*, 2012, pp. 3541–3548.

[24] E. Orietti, P. Mattavelli, G. Spiazzi, C. Adragna, and G. Gattavari, "Two-phase interleaved LLC resonant converter with current-controlled inductor," in *Proc. Brazilian Power Electron. Conf.*, 2009, pp. 298–304.

[25] B. C. Kim, K. B. Park, C. E. Kim, and G. W. Moon, "Load sharing characteristic of two-phase interleaved LLC resonant converter with parallel and series input structure," in *Proc. IEEE Energy Convers. Congr. Expo.*, 2009, pp. 750–753.

[26] F. Jin, F. Liu, X. Ruan, and X. Meng, "Multi-phase multi-level LLC resonant converter with low voltage stress on the primary-side switches," in *Proc. IEEE Energy Convers. Congr. Expo.*, 2014, pp. 4704–4710.

[27] E. Orietti, P. Mattavelli, G. Spiazzi, C. Adragna, and G. Gattavari, "Analysis of multi-phase LLC resonant converters," in *Proc. Brazilian Power Electron. Conf.*, 2009, pp. 464–471.

[28] E. Orietti, P. Mattavelli, G. Spiazzi, C. Adragna, and G. Gattavari, "Current sharing in three-phase LLC interleaved resonant converter," in *Proc. IEEE Energy Convers. Congr. Expo.*, 2009, pp. 1145–1152.

[29] H. Wang, Y. Chen, Y.-F. Liu, J. Afsharian, and A. Z. Yang, "A common inductor multi-phase LLC resonant converter," in *Proc. IEEE Energy Convers. Congr. Expo.*, 2015, pp. 548–555.

[30] H. Wang *et al.*, "A common capacitor multi-phase LLC resonant converter," in *Proc. IEEE Appl. Power Electron. Conf. Expo.*, 2016, pp. 2320–2327.

[31] H. Wang *et al.*, "An algorithm to analyze circulating current for multi-phase resonant converter," in *Proc. IEEE Appl. Power Electron. Conf. Expo.*, 2016, pp. 899–906.

[32] H. Wang, Y. Chen, and Y. F. Liu, "A passive-impedance-matching concept for multiphase resonant converter," in *Proc. IEEE Appl. Power Electron. Conf. Expo.*, 2016, pp. 2304–2311.

[33] H. Wang, Y. Chen, Y. F. Liu, J. Afsharian, and Z. Yang, "A passive current sharing method with common inductor multi-phase LLC resonant converter," *IEEE Trans. Power Electron.*, to be published.

[34] I. O. Lee and G. W. Moon, "The k-Q analysis for an LLC series resonant converter," *IEEE Trans. Power Electron.*, vol. 29, no. 1, pp. 13–16, Jan. 2014.

[35] X. Chen, D. Huang, Q. Li, and F. C. Lee, "Multi-channel LED driver with CLL resonant converter," in *Proc. IEEE Energy Convers. Congr. Expo.*, 2014, pp. 3599–3606.

[36] D. Huang, D. Fu, F. C. Lee, and P. Kong, "High-frequency high-efficiency CLL resonant converters with synchronous rectifiers," *IEEE Trans. Ind. Electron.*, vol. 58, no. 8, pp. 3461–3470, Aug. 2011.
[37] X. Chen, D. Huang, Q. Li, and F. C. Lee, "Multichannel LED driver with CLL resonant converter," *IEEE J. Emerg. Sel. Topics Power Electron.*, vol. 3, no. 3, pp. 589–598, Sep. 2015.
[38] J. L. Sosa, M. Castilla, J. Miret, L. G. D. Vicuna, and L. S. Moreno, "Sliding-mode input-output linearization controller for the DC/DC ZVS CLL-T resonant converter," *IEEE Trans. Ind. Electron.*, vol. 59, no. 3, pp. 1554–1564, Mar. 2012.
[39] D. Czarkowski and M. K. Kazimierczuk, "Phase-controlled CLL resonant converter," in *Proc. 18th Annu. Appl. Power Electron. Conf. Expo.*, 1993, pp. 432–438.
[40] C. Chakraborty, M. Ishida, and T. Hori, "Performance, design and pulse width control of a CLL resonant DC/DC converter operating at constant frequency in the lagging power factor mode," in *Proc. IEEE Int. Conf. Power Electron. Drive Syst.*, 1999, vol. 2, pp. 767–772.

Hongliang Wang (M'12–SM'15) received the B.Sc. degree in electrical engineering from Anhui University of Science and Technology, Huainan, China, in 2004, and the Ph.D. degree in electrical engineering from Huazhong University of Science and Technology, Wuhan, China, in 2011.

From 2004 to 2005, he was an Electrical Engineer with Zhejiang Hengdian Thermal Power Plant. From 2011 to 2013, he was a Senior System Engineer with Sungrow Power Supply Co., Ltd. He has been a Postdoctoral Fellow at Queen's University, Kingston, ON, Canada, since 2013. He has authored or coauthored more than 50 papers in conferences and journals. He is the inventor/coinventor of 41 China-issued patents, 15 U.S. patents, and six PCT patents pending. His research interests include power electronics, including digital control, modulation, and multilevel topology of the inverter for photovoltaic application and microgrid application, resonant converters and server power supplies, and LED drivers.

Dr. Wang is a Senior Member of the China Electro-Technical Society, a senior member of the China Power Supply Society (CPSS). He serves as a member of the CPSS Technical Committee on Standardization, a member of the CPSS Technical Committee on Renewable Energy Power Conversion, the Vice-Chair of Kingston Section of the IEEE, a Session Chair of the 2015 IEEE Energy Conversion Congress and Exposition, a TPC Member of the 2012 International Conference on Electrical Machines and Systems, and a China Expert Group Member of IEC standard TC8/PT 62786.

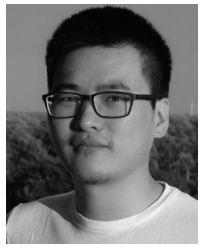

Yang Chen (S'14) received the B.Sc. and the M.Sc. degrees in electrical engineering from Beijing Institute of Technology, Beijing, China, in 2011 and 2013, respectively. He is currently working toward the Ph.D. degree at Queen's University, Kingston, ON, Canada.

His research interests include topology, control, and design of resonant converters in ac–dc and dc–dc fields, power factor correction technology, and digital control.

Yan-Fei Liu (M'94–SM'97–F'13) received the bachelor's and master's degrees in electrical engineering from Zhejiang University, Hangzhou, China, in 1984 and 1987, respectively, and Ph.D. degree in electrical and computer engineering from Queen's University, Kingston, ON, Canada, in 1994.

He was a Technical Advisor with the Advanced Power System Division, Nortel Networks, Ottawa, ON, from 1994 to 1999. Since 1999, he has been with Queen's University, where he is currently a Professor with the Department of Electrical and Computer Engineering. He has authored more than 200 technical papers in the IEEE Transactions and conferences and holds 20 U.S. patents. He is also a Principal Contributor for two IEEE standards. His current research interests include digital control technologies for high-efficiency fast-dynamic-response dc–dc switching converters and ac–dc converters with power factor correction, resonant converters, and server power supplies, and LED drivers.

Dr. Liu received the Premier's Research Excellence Award in 2000 in Ontario, ON. He also received the Award of Excellence in Technology in Nortel in 1997. He has been an Editor of the IEEE JOURNAL OF EMERGING AND SELECTED TOPICS OF POWER ELECTRONICS (IEEE JESTPE) since 2013 and an Associate Editor for the IEEE TRANSACTIONS ON POWER ELECTRONICS since 2001,. He was a Guest Editor-in-Chief for the special issue of Power Supply on Chip of the IEEE TRANSACTIONS ON POWER ELECTRONICS from 2011 to 2013. He also served as the Guest Editor for special issues of the IEEE JESTPE: Miniaturization of Power Electronics Systems in 2014 and Green Power Supplies in 2016. He serves as the co-General Chair of the 2015 IEEE Energy Conversion Congress and Exposition (ECCE) held in Montreal, QC, Canada, in September 2015. He will be the General chair of ECCE 2019 to be held in Baltimore, MD, USA. He has been the Chair of the PELS Technical Committee on Control and Modeling Core Technologies since 2013 and was the chair of the PELS Technical Committee on Power Conversion Systems and Components from 2009 to 2012.